



Longitudinal top polarisation measurement and anomalous Wtb coupling

V. Arun Prasath^{1,a}, Rohini M. Godbole^{1,b}, Saurabh D. Rindani^{2,c}

¹ Centre for High Energy Physics, Indian Institute of Science, Bangalore 560 012, India

² Physical Research Laboratory, Navarangpura, Ahmedabad 380 009, India

Received: 15 December 2014 / Accepted: 5 August 2015

© The Author(s) 2015. This article is published with open access at Springerlink.com

Abstract Kinematical distributions of decay products of the top quark carry information on the polarisation of the top as well as on any possible new physics in the decay of the top quark. We construct observables in the form of asymmetries in the kinematical distributions to probe their effects. Charged-lepton angular distributions in the decay are insensitive to anomalous couplings to leading order. Hence these can be a robust probe of top polarisation. However, these are difficult to measure in the case of highly boosted top quarks as compared to energy distributions of decay products. These are then sensitive, in general, to both top polarisation and top anomalous couplings. We compare various asymmetries for their sensitivities to the longitudinal polarisation of the top quark as well as to possible new physics in the Wtb vertex, paying special attention to the case of highly boosted top quarks. We perform a χ^2 analysis to determine the regions in the plane of longitudinal polarisation of the top quark and the couplings of the Wtb vertex constrained by different combinations of the asymmetries. Moreover, we find that the use of observables sensitive to the longitudinal top polarisation can add to the sensitivity to which the Wtb vertex can be probed.

1 Introduction

The top quark is the heaviest of all fundamental particles discovered so far in the standard model (SM). Since the mass of the top quark ($m_t = 173.5 \text{ GeV}/c^2$) [1] is very close to the electroweak symmetry breaking (EWSB) scale, effects of any new physics (NP) associated with EWSB are likely to reveal themselves in the properties of the top quark. The LHC, during the course of its runs, is expected to determine several of the properties of the top quark [2–7]. A comparison of these

with expectations from the SM will reveal NP, if present. In the search for NP, there are already some results from the LHC, which include those on the top-quark polarisation and anomalous couplings in the Wtb vertex [8, 9], which are relevant to the discussion in this paper.

New physics may appear in the production of the top quark or its decay or both (see for example [10–19]). A model-independent way of probing NP in the top sector is provided by the effective-theory formalism where all gauge-invariant higher-dimensional operators suppressed by powers of the corresponding scale of NP are added to the SM Lagrangian [20–25]. This description is valid at scales much lower than the NP scale. A complete set of dimension-six operators relevant to top production and decay can be found in [25]. Higher order effects within the SM itself could induce structures that are not present at the tree-level vertex (see for example [26–29]).

The top quark, on account of its large mass, decays before it hadronises, thereby transferring its spin information to the decay products. The angular and energy distributions of the decay products carry information on the spin of the top quark [30–33]. Kinematic distributions of the decay products of the top in the presence of anomalous couplings have been studied, without assuming any model, in [34–37]. The effects of higher order QCD corrections on the distributions are studied in [26, 30, 31, 38–45].

The polarisation of top quarks produced in a hadron collider like the LHC depends upon the hard subprocesses that produce them. Since QCD which is mainly responsible for top-pair production in the SM is a vector interaction, there is no significant longitudinal polarisation of the top quarks pair produced in the SM: less than about a percent, after taking into account the one loop electroweak radiative corrections, in the so-called helicity basis¹ defined in $t\bar{t}$ centre of mass

^a e-mail: arunprasath@cts.iisc.ernet.in

^b e-mail: rohini@cts.iisc.ernet.in

^c e-mail: saurabh@ppl.res.in

¹ The helicity basis is defined as the basis in which the top spin quantisation axis is taken along the direction of motion of the top.

(c.m.) frame of pp collisions at the LHC [46–49]. Single-top production, occurring via electroweak interactions at much lower rates, does give rise to polarised top quarks [50,51]. The value of polarisation after including NLO QCD corrections is ~ 0.91 in the helicity basis defined in the c.m. frame of the top quark and the spectator jet (the jet from the light quark that is scattered away along with the top) [51]. Note that the top can be polarised along a direction that is perpendicular to the plane of production of the top (‘transverse polarisation’). While in the SM longitudinal polarisation requires parity violating interactions, transverse polarisation is allowed even when the interactions are parity conserving as in the case of QCD. This, however, is generated only at one loop level in QCD. In the case of top pair production, it does not exceed $\sim 2\%$ at the parton level [32,52,53]. This value is further reduced at the LHC due to the dominance of the gluon-fusion channel in $t\bar{t}$ production: $\sim 0.2\%$ at 7 TeV [54]. In this work, we focus only on the longitudinal polarisation. Hence, in our paper the term top polarisation always refers to the longitudinal polarisation unless it is explicitly stated otherwise.

Since the standard model value of top polarisation in top pair production is small, the observation of a substantial polarisation in top-pair production will strongly indicate NP. Any nontrivial chiral structure in the top coupling induced by the NP can affect the polarisation of the produced top quarks [19,55–66]. Hence measurement of the polarisation of the top quark can provide information on the chiral structure of the couplings involved in NP contributions to top quark-production [55–65,67–71].

New physics reflects itself in changes in the total and differential cross sections for top production. The detailed study of angular distributions of the decay products of the top quark, which are also affected by top-quark polarisation, provides a useful handle for the discrimination between different NP models. Moreover, when NP couplings are small and the deviations of the total cross section from theoretical predictions in the SM can be small, the kinematic distributions and final-state polarisations being sensitive to the interference between the SM contribution and NP contribution can lead to increased sensitivity. The top-quark polarisation can, in addition, give a handle on the chiral structure of the couplings in NP.

A number of interesting scenarios for the production of top quarks occur once extensions of the standard model are introduced. The most popular extensions include supersymmetry, theories with extra dimensions and theories with extended gauge groups, all of which introduce new particles, which would contribute to top quark production in various ways: through an on shell production of resonances or via virtual effects. As said before, a nontrivial chiral structure of the top-quark couplings induced by the NP will lead to a prediction for top-quark polarisation which depends on the values of

the parameters of that particular extension of the SM being considered.

Some of the NP models predict new heavy resonances with masses at the TeV scale [72–74]. Such heavy resonances are produced effectively at rest in the parton centre-of-mass (cm) frame. When these heavy resonances decay into top quarks, the resulting top quarks are highly boosted in the lab frame. The decay products of these highly boosted top quarks are collimated along the direction of motion of the parent top quark. In such a case observables based on the energy distributions of the decay products rather than their angular distributions are more suitable to probe the polarisation of the top quark [75]. For such highly boosted tops methods based on the jet substructure have been proposed to extract information on the polarisation of the top which then can be used to get information on the production mechanism of top quarks [76–78]. Recently a new method for measuring the polarisation of top, when the top decays hadronically, has been proposed [79]. This method, involving a weighted average, in the top rest frame, of the directions of two light-quark jets that come from the decay $t \rightarrow bj\bar{j}$, has been shown to perform better than methods based on other hadronic top spin analysers.

Data from the LHC has placed stringent lower bounds on the masses of resonances [80–84]. If they do exist at higher masses, the observation in the invariant mass distribution would be difficult. On the other hand, NP production amplitude of the resonance giving rise to a top pair could have sizable interference with the SM amplitude. This could lead to observable top polarisation provided the NP couplings have a nontrivial chiral structure. Top polarisation can serve as a tool in testing these models [58,59].

Another example of significant top polarisation is in stop decay,

$$\tilde{t}_1 \rightarrow t\tilde{\chi}_i^0, \quad (1)$$

in the minimal supersymmetric standard model (MSSM), where \tilde{t}_1 is the lightest stop and $\tilde{\chi}_i^0, i = 1, \dots, 4$ stand for the four neutralinos, which can be used to study mixing in the sfermion sector as well as the neutralino–chargino sector [56,63,64,85]. In R -parity violating MSSM, top quark pairs produced via a t -channel exchange of a stau, or a stop or a top quark produced in association with a slepton, can have nonzero polarisation, whose measurement can be used to constrain the R -parity violating couplings [57,86,87]. There have been several NP explanations of the forward–backward asymmetry of the top quark observed at Tevatron (see, for example [54,88–110]), and top polarisation can be useful in discriminating among them [68,69,111,112]. In fact the top polarisation transverse to the $t\bar{t}$ production plane also could be used to test whether the measured forward–backward asymmetry at the Tevatron is due to the effect of some NP in

the top pair production [54], even when the NP is difficult to observe directly.

Since the top quark mainly decays through the channel $t \rightarrow Wb$ with a branching ratio of $\approx 100\%$, any new physics which appears through the Wtb vertex can affect the measurement of the polarisation of top quarks which is determined by the production process. In general, measures of top polarisation have a dependence both on the strength and the tensor structure of the Wtb coupling associated with top decay. Measures of top polarisation which depend only on the energy integrated angular distributions are insensitive to the anomalous part of the decay vertex Wtb [36, 37, 113–115]. Recently another measure of top-quark polarisation has been proposed in [116] which factors out the effect of any possible anomalous Wtb vertex from the polarisation of the top quark. The factor which contains the information about the Wtb vertex of the top decay can be extracted in a model-independent way from the angular distributions of the top quark's decay products [117]. Since the anomalous tbW coupling also affects the kinematic distributions of the decay products of the top quark, it too can be probed by studying these and such probes have been constructed [61, 117–126]. Probing anomalous Wtb couplings at future colliders such as LHeC and ILC have also been considered by various authors [127–130].

Since the NP can affect top polarisation as well as give rise to anomalous decay vertex, it is of interest to explore how well one can study simultaneously both the top polarisation and the anomalous Wtb couplings and further see how probes of one are influenced by the other. We present in this note some observations on construction of various observables as a measure of top polarisation and how one can simultaneously probe top polarisation and the anomalous Wtb coupling, when neither of the two is known a priori.

Studies of spin effects in top physics have largely concentrated on spin correlations in top pair production, as these are nonzero even in the SM and the measurements are interesting, even if no NP effects exist. A comparison of experimental results with SM predictions can then be used to constrain the NP models. The results so obtained at the Tevatron and the LHC have so far shown consistency with the SM, though errors are large. These correlations are best measured using leptonic final states from both top and anti-top. It is conceivable that a single polarisation measurement on either the top or the anti-top which decays leptonically, allowing the other to decay hadronically, could add to the accuracy.

Moreover, attempts to measure single-top polarisation at the Tevatron and at the LHC have so far been made by reconstructing the rest frame of the top quark. A method which does not require such full reconstruction of the top may be desirable. We have thus concentrated on the measures of the polarisation of a single top in the laboratory frame.

We construct various kinematic observables (asymmetries), make a comparative study of their dependence on top polarisation and anomalous Wtb vertex, and examine the possibility of simultaneously constraining the anomalous Wtb vertex and the polarisation of the top quark. Our observables do not always require full reconstruction of the top momentum. We do not look at any specific top production mechanism, but simply consider the top quark to be produced in the lab frame with various momenta, paying special attention to highly boosted top quarks.

Our paper below is divided into four sections. In Sect. 2 we describe the structure of Wtb vertex and constraints on various anomalous couplings. In Sect. 3 we make a comparative study of the sensitivities of different asymmetries to the polarisation of the top and anomalous Wtb couplings. In Sect. 4 we use these asymmetries to constrain simultaneously the polarisation of the top quark and the Wtb vertex. In Sect. 5 we give a summary and conclusions.²

2 The structure of Wtb vertex

The Wtb vertex in the SM has a $V - A$ structure. Depending upon the NP the structure of Wtb vertex can be modified from the $V - A$ structure (see, for example [131]). We follow a model-independent approach by writing down the most general Wtb vertex [117]:

$$\Gamma^\mu = -i \frac{g}{\sqrt{2}} \left[\gamma^\mu (f_{1L} P_L + f_{1R} P_R) - \frac{i}{M_W} \sigma^{\mu\nu} (p_t - p_b)_\nu (f_{2L} P_L + f_{2R} P_R) \right] \quad (2)$$

where g is the $SU(2)_L$ gauge coupling constant, p_t , p_b are the four-momenta of the top and the bottom quarks respectively, and P_L , P_R are the left and right chiral projectors. In the SM, $f_{1L} = 1$ and $f_{1R} = f_{2L} = f_{2R} = 0$ at tree level. One loop QCD contributions to the Wtb vertex have been computed within the SM, in [27, 28, 39]. Electroweak corrections also affect the Wtb vertex and in turn affect the couplings $f_{1L,R}$ and $f_{2L,R}$. One loop EW contributions to the tensor couplings amount to about 10 % of the one loop QCD contributions [29]. After including the EW contributions the tensor couplings at one loop level in the SM are as follows: $f_{2L} = -(1.21 + 0.01i) \times 10^{-3}$ and $f_{2R} = -(7.17 + 1.23i) \times 10^{-3}$ [29].

² In this work all kinematic quantities in the rest frame of the top quark are denoted by a subscript '0'. All kinematic quantities which do not have subscript '0' are in the laboratory frame (lab frame), unless stated otherwise. We have assumed that the top quark has spin along the direction of motion of the top in the lab frame. The lab frame polarisation is obtained from the rest frame one by a boost along the direction of motion of the top quark. We use the word lepton to denote the charged anti-lepton $\bar{\ell}$ from $t \rightarrow b\bar{\ell}\nu$.

We take the CKM matrix element $V_{tb} \approx 1$. Similarly, the vertex $\bar{t}W\bar{b}$ with anomalous couplings is given by

$$\Gamma^\mu = -i \frac{g}{\sqrt{2}} \left[\gamma^\mu (\bar{f}_{1L} P_L + \bar{f}_{1R} P_R) - \frac{i}{M_W} \sigma^{\mu\nu} (p_t - p_b)_\nu (\bar{f}_{2L} P_L + \bar{f}_{2R} P_R) \right]. \quad (3)$$

When CP is conserved, $f_{1L} = \bar{f}_{1L}$, $f_{1R} = \bar{f}_{1R}$, $f_{2L} = \bar{f}_{2R}$ and $f_{2R} = \bar{f}_{2L}$ [126]. Direct searches of NP in top decay at the Tevatron give constraints on the coefficients: $|f_{1R}|^2 < 0.30$, $|f_{2L}|^2 < 0.05$, $|f_{2R}|^2 < 0.12$ at 95 % confidence level (C.L.) assuming $f_{1L} = 1$ [132]. Indirect constraints from the measurement of the branching ratio of $b \rightarrow s\gamma$ are stronger for f_{1R} , f_{2L} and weaker for f_{2R} : $-0.15 \leq \text{Re}(f_{2R}) \leq 0.57$, $-0.0007 \leq f_{1R} \leq 0.0025$, $-0.0013 \leq f_{2L} \leq 0.0004$ [133] at 95 % C.L. Direct search constraints are given also by the LHC: for $f_{1L} = 1$, $f_{1R} = f_{2L} = 0$ the CMS collaboration [9] obtained as a best fit value of the tensor part of the Wtb coupling which in our notation reads as $f_{2R} = 0.070 \pm 0.053$ (stat) $^{+0.081}_{-0.073}$ (syst) in a fit to measured W helicity fractions proposed by [32]. A combination of data from the Tevatron, and the LHC on observables like the t -channel single top cross section, and the W helicity fractions, gives, in our sign conventions, $-0.11 \leq \text{Re}(f_{2R}) \leq 0.13$ and $-0.31 \leq \text{Im}(f_{2R}) \leq 0.31$ respectively at 95 % C.L. [134]. When CP is conserved, the constraints on the anomalous couplings \bar{f}_{1L} , \bar{f}_{1R} , \bar{f}_{2L} and \bar{f}_{2R} are the same as those for f_{1L} , f_{1R} , f_{2R} and f_{2L} respectively.

In the analytical expressions for different kinematic distributions (see below) we have assumed that the anomalous couplings f_{1L} and \bar{f}_{1L} are real valued while all other anomalous couplings are complex valued. However, in view of the strong constraints on the anomalous couplings, in our numerical work and in analytical results on Wtb vertex, we set $f_{1R} = f_{2L} = 0$. In numerical works, we also set $f_{1L} = 1$ and take f_{2R} as a real valued quantity varying in the range -0.2 to $+0.2$.

3 Kinematic distributions of the decay products of the top

Recall that a measurement of the polarisation of the top quark can only be done through the kinematic distributions of its decay products and these would also be affected by the nature of the Wtb coupling.

We begin by looking at the details of the three-body decay of the top quark. The top quark decays into a b quark and a W boson which in turn decays into a charged anti-lepton ($\bar{\ell}$) and a neutrino ν_ℓ . We assume that all the particles in the decay chain $t \rightarrow bW \rightarrow b\bar{\ell}\nu_\ell$ are on-shell (including the intermediate W boson). The angular distributions of the

decay products are correlated to the polarisation P of the top quark. In the SM, in the rest frame of the top quark, the energy integrated distribution is given by

$$\frac{1}{\Gamma} \frac{d\Gamma}{d\cos\theta_X} = \frac{1}{2} (1 + P\alpha_X \cos\theta_X) \quad (4)$$

where $X = b, \ell, W, \nu_\ell$, the quantity α_X is called the spin-analysing power of the particle X and θ_X is the angle between the direction of the momentum of the particle X and the top quark spin axis in the rest frame of the top quark. The spin-analysing powers of the b quark, lepton and the neutrino in the SM at tree level are

$$\begin{aligned} \alpha_b &= -\left(\frac{\xi - 2}{\xi + 2}\right), \\ \alpha_\ell &= 1, \\ \alpha_\nu &= 1 - \frac{12\xi(\xi - 1 - \log\xi)}{(\xi - 1)^2(\xi + 2)}, \end{aligned}$$

respectively, where $\xi = \frac{m_t^2}{m_W^2}$ [135]. Higher order QCD effects on the spin-analysing power of the lepton ℓ are at the per-mille level [31]. But in the case of hadronic decay of the top, the QCD corrections to the spin-analysing powers of quarks from the top decay can be up to about 4 % [39,45].

3.1 Kinematics of the top decay

Before proceeding to the description of asymmetries, we give a brief description of the kinematics of the top quark decay: $t \rightarrow Wb \rightarrow b\bar{\ell}\nu$.

The conservation of energy and momentum and the on-shell condition of W give the following equations:

$$p_t = p_b + p_\ell + p_\nu \quad (5)$$

and

$$m_W^2 = (p_\ell + p_\nu)^2 \quad (6)$$

where p_t, p_b, p_ℓ, p_ν are the four-momenta of the particles. Solving these equations along with the on-shell condition of the particles fixes all but four variables in the rest frame of the top quark: energy of the lepton $E_{\ell,0}$, the polar and azimuthal angles of the lepton $\theta_{\ell,0}, \phi_{\ell,0}$ and the azimuthal angle (α_0) of the b quark with respect to a coordinate system where the z axis is along the direction of the lepton momentum. The variables fixed by Eqs. 5 and 6 and the on-shell conditions are the energy of the b quark, $E_{b,0} = (m_t^2 - m_W^2)/2m_t$ and the cosine of the angle between the b -quark momentum and the lepton momentum, $\cos\zeta = (2 - x_{\ell,0}(\xi + 1))/(x_{\ell,0}(\xi - 1))$ where $\xi = m_t^2/m_W^2$. The energy $E_{\ell,0}$ of the lepton is constrained to vary between $m_W^2/2m_t$ and $m_t/2$.

3.2 Definition of asymmetry

The asymmetry in a kinematic variable X is defined (in a given frame) as

$$A_X = \frac{\int_{X_{\min}}^{X_c} \frac{d\Gamma}{dX} dX - \int_{X_c}^{X_{\max}} \frac{d\Gamma}{dX} dX}{\int_{X_{\min}}^{X_c} \frac{d\Gamma}{dX} dX + \int_{X_c}^{X_{\max}} \frac{d\Gamma}{dX} dX} \quad (7)$$

where $\frac{d\Gamma}{dX}$ is the differential partial decay width of the top quark in the variable X and X_c is a value of X between $[X_{\min}, X_{\max}]$ chosen as a reference point about which the asymmetry is evaluated. In this work, we chose reference points on the basis of the following considerations:

1. The reference point should be such that the evaluated asymmetry is sensitive to both of the parameters P and f_{2R} throughout their allowed range of values. In other words, the asymmetries thus obtained should be able to distinguish between different values of the parameters.
2. The choice of the reference point should allow for a comparison of cases of different values of the parameters.

The asymmetries vary in their sensitivity to the polarisation of the top quark and the anomalous coupling f_{2R} , and in their usefulness in a particular kinematic regime of top decay. We describe four such asymmetries in this section. We can classify them into broadly two categories: angular asymmetries and energy-based asymmetries. Examples of the former include A_{θ_ℓ} and of the latter include A_{x_ℓ} , A_u , and A_z . When the top quarks are highly boosted, the decay products of the top are highly collimated. In this case measurement of angular distribution of visible decay products is possible but difficult [136]. Hence energy-based asymmetries are used to probe the top-quark polarisation [75] and Wtb vertex.

3.3 The θ_ℓ asymmetry (A_{θ_ℓ})

The asymmetry is defined in terms of $\cos \theta_\ell$ where θ_ℓ is the angle between the momentum of the lepton from the W decay and the top-quark direction of motion. The $\cos \theta_\ell$ -distribution is sensitive to the polarisation of the top quark (P). In the rest frame of the top quark the distribution is given in the SM by

$$\frac{1}{\Gamma} \frac{d\Gamma}{d \cos \theta_{\ell,0}} = \frac{1}{2} (1 + P \cos \theta_{\ell,0}). \quad (8)$$

This expression is valid even when the anomalous coupling f_{2R} is nonzero, provided it is small [36,37,113–115]. In the lab frame the $\cos \theta_\ell$ -distribution becomes [61]

$$\begin{aligned} \frac{1}{\Gamma} \frac{d\Gamma}{dt} &= \frac{(1 - \beta^2)}{2(1 - \beta t)^3 X} [(\xi - 1)^2 (f_{1L}^2 (\xi + 2) \\ &+ 6\sqrt{\xi} f_{1L} \text{Re}(f_{2R})) \{P(t - \beta) + (1 - \beta t)\} \\ &+ 12P\xi(t - \beta)|f_{2R}|^2(-\xi + 1 + \xi \log \xi) \\ &+ |f_{2R}|^2(\xi - 1)^2(2\xi + 1)\{(1 - \beta t) - P(t - \beta)\}] \end{aligned} \quad (9)$$

where $t = \cos \theta_\ell$ is the cosine of the angle between the top-quark direction of motion and the lepton momentum in the lab frame. In Eq. 9, the factor X in the denominator of the right-hand side is given by

$$\begin{aligned} X &= (\xi - 1)^2 [(\xi + 2)f_{1L}^2 + 6\sqrt{\xi} f_{1L} \text{Re}(f_{2R}) \\ &+ (2\xi + 1)|f_{2R}|^2] \end{aligned} \quad (10)$$

and β is the boost required to go from the lab frame to the top-quark rest frame. When $|f_{2R}| \ll 1$, keeping only terms which are first order in f_{2R} , we get

$$\frac{1}{\Gamma} \frac{d\Gamma}{dt} \sim \frac{(1 - \beta^2)}{2(1 - \beta t)^3} ((1 - \beta P) + (P - \beta)t), \quad (11)$$

which is completely independent of the anomalous coupling f_{2R} . In other words, the energy-integrated distribution $1/\Gamma d\Gamma/d \cos \theta_\ell$ is only very very weakly dependent on the anomalous coupling f_{2R} .

Therefore the lepton angular asymmetry (A_{θ_ℓ}) serves as a useful measure of polarisation of the top quark irrespective of NP effects at the decay vertex when they are small [36].

In the SM, the asymmetry about the point $\cos \theta_\ell = 0$ is given in the lab frame, using Eq. 7, by

$$A_{\theta_\ell} = \frac{1}{2} (-2\beta + P(-1 + \beta^2)). \quad (12)$$

From this equation one can easily observe that the sensitivity of A_{θ_ℓ} to the polarisation of the top quarks decreases with increasing boost. This can be understood as follows: in the rest frame of the top quark, the lepton is preferentially emitted either in the forward direction or the backward direction depending upon the sign of the polarisation of the top quark (P) (Eq. 8). But in the lab frame, at large values of boost, the lepton emission is strongly suppressed except in the direction $\cos \theta_\ell = 1$ due to kinematics which appears through the factor $(1 - \beta^2)/(1 - \beta t)^3$ in Eq. 9 for all values of polarisation P . This means that the lepton angular distribution loses its sensitivity to P at large boosts as shown in Eq. 12.

3.4 The x_ℓ asymmetry (A_{x_ℓ})

The variable x_ℓ is defined as $x_\ell = 2E_\ell/m_t$ where E_ℓ is the energy of the lepton from the top decay in a given frame. Unlike the $\theta_{\ell,0}$ -distribution, the $x_{\ell,0}$ distribution is not insensitive to f_{2R} in the top quark rest frame. The analytical expression for the distribution $(1/\Gamma)d\Gamma/dx_{\ell,0}$, in the top quark rest frame, is given by

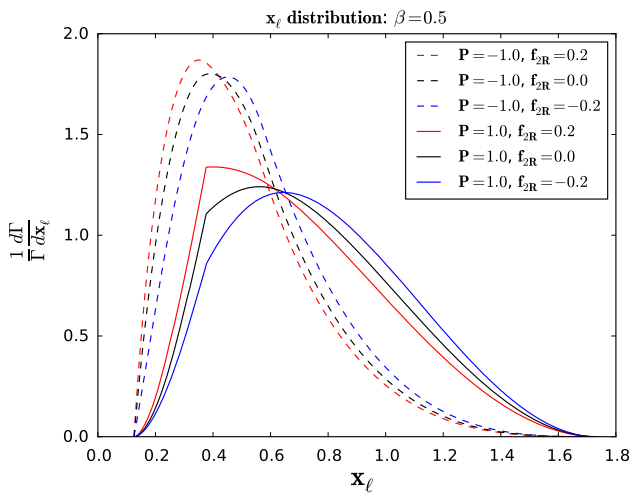


Fig. 1 The x_ℓ -distribution in the lab frame for different values of the polarisation of the top quark (P) and the anomalous coupling (f_{2R})

$$\frac{1}{\Gamma} \frac{d\Gamma}{dx_{\ell,0}} = 6\xi^2 \frac{1}{X} (1 - x_{\ell,0}) [f_{1L}^2 \xi x_{\ell,0} + f_{1L} \text{Re}(f_{2R}) \sqrt{\xi} + |f_{2R}|^2 (\xi + 1 - x_{\ell,0} \xi)] \quad (13)$$

where X is given in Eq. 10. In the case when $|f_{2R}| \ll 1$ the distribution is not independent of f_{2R} as the factors that are linear in f_{2R} do not cancel each other from the denominator and the numerator of Eq. 13. The distribution $1/\Gamma d\Gamma/dx_\ell$ is plotted in Fig. 1 for different values of the top polarisation P and the anomalous coupling f_{2R} . The location of the peak of the distribution for a given top polarisation P depends upon the anomalous coupling f_{2R} as can be seen from the figure. The sharp edges in the distribution for $P = 1$ appear due to the interplay of the polarisation of the top and the kinematics of the top decay.

It would be convenient if the value of x_ℓ at the position of the peak is chosen as the reference point to evaluate the asymmetry A_{x_ℓ} . In view of the fact that this point varies with P as well as f_{2R} , for uniformity we take the value of x_ℓ corresponding to the peak of the distribution for $P = -1$ and $f_{2R} = 0$ as a reference point for all values of P and f_{2R} . This choice is consistent with our method of choosing the reference points as given in Sect. 3.2.

The above equation also shows that the $x_{\ell,0}$ -distribution is independent of P in the rest frame of the top quark. Therefore the asymmetry $A_{x_{\ell,0}}$ has no sensitivity to the polarisation of the top quark (P) in the top quark rest frame. But under a Lorentz transformation along the top-quark direction of motion which takes the top quark rest frame to the lab frame, the energy of the lepton in the lab frame gets related to both the energy and the polar angle $\theta_{\ell,0}$ of the lepton measured in the top quark rest frame:

$$E_\ell = \frac{1}{\sqrt{1 - \beta^2}} E_{\ell,0} (1 + \beta \cos \theta_{\ell,0}).$$

Since the distribution in $\theta_{\ell,0}$ is correlated to the top-quark polarisation (P) (see Eq. 8), the distribution in E_ℓ (or x_ℓ) becomes dependent on P . Hence the asymmetry A_{x_ℓ} for $\beta \neq 0$ depends on the polarisation of the top quark (P).

A variable similar to x_ℓ has been proposed in [137]. It is defined as $x_B = 2E_\ell/E_t$ and it is related to x_ℓ by a boost dependent factor: $x_B = \sqrt{1 - \beta^2} x_\ell / 2$. However, the asymmetry constructed out of x_B -distribution is the same as the asymmetry A_{x_ℓ} at any given value of β .

3.5 The u asymmetry (A_u)

The variable u is defined as $u = E_\ell / (E_\ell + E_b)$ where E_ℓ and E_b are the energies in the lab frame carried by the lepton and the b quark, respectively [75]. The variable u can be written as

$$u = \frac{\xi x_{\ell,0} (1 + \beta \cos \theta_{\ell,0})}{\xi x_{\ell,0} (1 + \beta \cos \theta_{\ell,0}) + (\xi - 1) (1 + \beta \cos \theta_{b,0})} \quad (14)$$

where $x_{\ell,0} = 2E_{\ell,0}/m_t$, $E_{\ell,0}$ and $\theta_{\ell,0}$ are the energy and the angle between the top quark direction of motion and the momentum of the lepton measured in the top quark rest frame respectively. $\cos \theta_{b,0}$ is given by

$$\cos \theta_{b,0} = -\sin \theta_{\ell,0} \sin \zeta \cos \alpha_0 + \cos \theta_{\ell,0} \cos \zeta \quad (15)$$

with $\cos \zeta = \frac{2 - x_{\ell,0}(\xi + 1)}{x_{\ell,0}(\xi - 1)}$ and $0 \leq \alpha_0 \leq 2\pi$, $(1/\xi) \leq x_{\ell,0} \leq 1$. u varies in the range (0, 1). The u -distribution is given by

$$\begin{aligned} \frac{1}{\Gamma} \frac{d\Gamma}{du} = & \int_0^\pi \int_{1/\xi}^1 dx_{\ell,0} d\theta_{\ell,0} \sum_{\alpha_{0,i}} \frac{1}{J(\alpha_{0,i})} \left(\frac{3\xi^2}{2\pi} \right) \frac{1}{X} \sin \theta_{\ell,0} \\ & \times (1 - x_{\ell,0}) [f_{1L}^2 \xi x_{\ell,0} (1 + P \cos \theta_{\ell,0}) \\ & + f_{1L} \text{Re}(f_{2R}) \sqrt{\xi} [P x_{\ell,0} (\cos \theta_{b,0} (\xi - 1) \\ & + \cos \theta_{\ell,0} (\xi + 1)) + 2] + |f_{2R}|^2 (\cos \theta_{b,0} P (\xi - 1) \\ & + \cos \theta_{\ell,0} P \xi x_{\ell,0} + \xi + 1 - x_{\ell,0} \xi)] \end{aligned} \quad (16)$$

where X is as defined in Eq. 10, and $\alpha_{0,i}$, ($i = 1, 2$) are the roots of the equation $u = u(x_{\ell,0}, \theta_{\ell,0}, \alpha_0)$.

Since u is invariant under the transformation $\alpha_0 \rightarrow 2\pi - \alpha_0$, we have two solutions: $\alpha_{0,1}$ and $2\pi - \alpha_{0,1}$ with $0 \leq \alpha_{0,1} \leq \pi$. The function $J(\alpha_{0,i})$ is given by

$$J(\alpha_{0,i}) = -\frac{u^2 (\xi - 1) \beta \sin \theta_{\ell,0} \sin \zeta \sin \alpha_{0,i}}{x_{\ell,0} \xi (1 + \beta \cos \theta_{\ell,0})} \quad (17)$$

where

$$\begin{aligned} \cos \alpha_{0,i} = & \frac{(1 + \beta \cos \theta_{\ell,0} \cos \zeta)}{\beta \sin \theta_{\ell,0} \sin \zeta} \\ & - \frac{(1/u - 1) \xi x_{\ell,0} (1 + \beta \cos \theta_{\ell,0})}{(\xi - 1) \beta \sin \theta_{\ell,0} \sin \zeta}. \end{aligned} \quad (18)$$

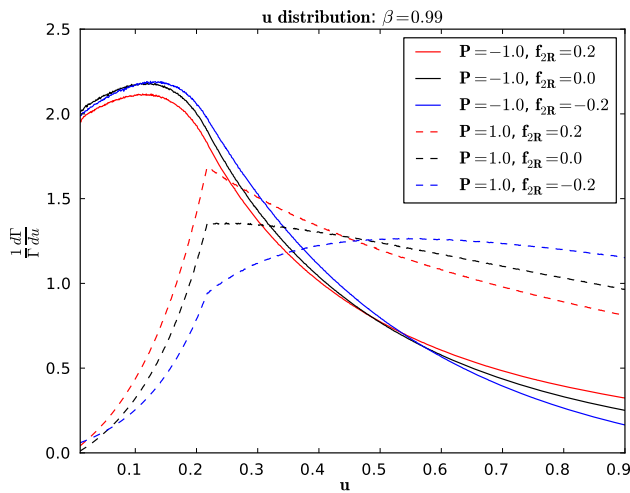


Fig. 2 The u -distribution as a function of the polarisation of the top quark (P) and the anomalous coupling f_{2R}

This equation determines $\alpha_{0,i}$, which can be used to get the value of the distribution at u . The asymmetry A_u is calculated for the point $u = u_c = 0.5$ using Eq. 7.

We note that the u -distribution is independent of $\text{Im}(f_{2R})$ to linear order: the integrand of Eq. 16 actually has an additional term that is proportional to $P(1 - x_\ell)x_\ell \sin \alpha \sin \theta_\ell \sin \zeta$. Since the u -distribution is obtained after summing over two values, i.e. $\alpha_{0,1}$ and $2\pi - \alpha_{0,1}$, this additional term does not give any contribution.

The u -distribution for different values of P and f_{2R} is given in Fig. 2. Similar to the case of the x_ℓ -distribution, the u -distribution has sharp edges for the same reasons given in Sect. 3.4.

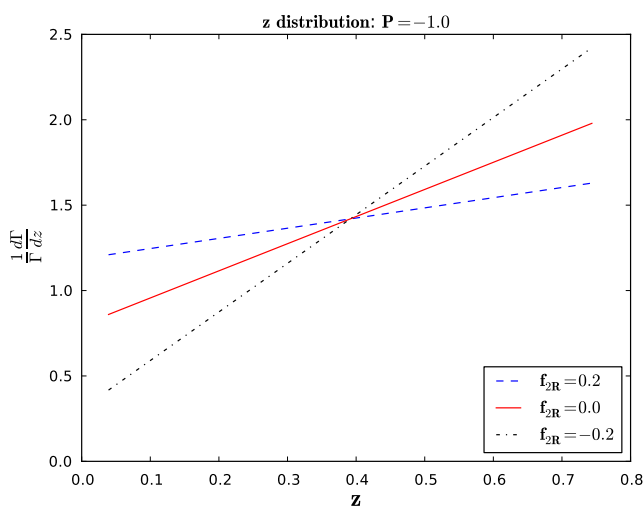


Fig. 3 The z -distribution $1/\Gamma d\Gamma/dz$ is plotted as a function of z for different values of f_{2R} . The left (right) figure corresponds to the polarisation of the top quark $P = -1.0$ ($P = 1.0$). The different lines show

3.6 The z asymmetry (A_z)

The variable z is defined as $z = E_b/E_t$ where E_b and E_t are the energies in the lab frame carried by the b and t quarks, respectively [75]. The variable z can be related to the variables defined in the rest frame of the top quark:

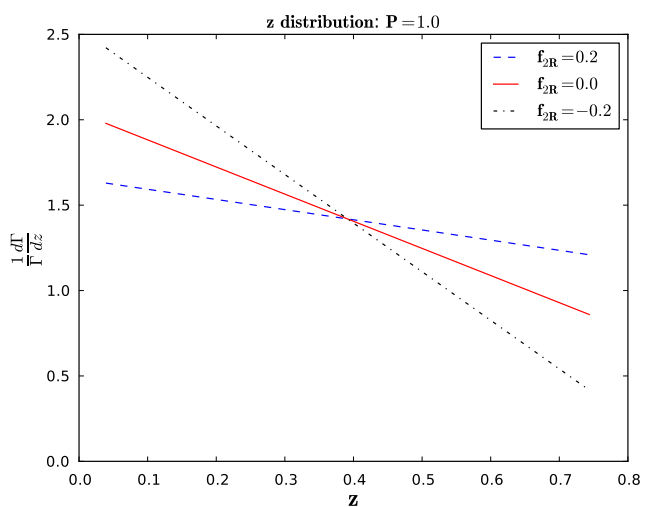
$$z = \frac{(\xi - 1)}{2\xi}(1 + \beta \cos \theta_{b,0}) \quad (19)$$

where $\cos \theta_{b,0}$ is as defined in Eq. 15. Since $\cos \theta_{b,0}$ varies in the range $[-1.0, 1.0]$, the variable z varies in the range $[(1 - \beta)(\xi - 1)/2\xi, (1 + \beta)(\xi - 1)/2\xi]$. The z -distribution is given by

$$\begin{aligned} \frac{1}{\Gamma} \frac{d\Gamma}{dz} = \frac{\xi}{\beta^2} \frac{1}{X} & [\beta(\xi - 1)\{f_{1L}^2(\xi + 2) \\ & + 6\sqrt{\xi} f_{1L} \text{Re}(f_{2R}) + |f_{2R}|^2(2\xi + 1)\} \\ & + P(-\xi + 1 + 2z\xi)\{-f_{1L}^2(\xi - 2) \\ & + 2\sqrt{\xi} f_{1L} \text{Re}(f_{2R}) + |f_{2R}|^2(2\xi - 1)\}]. \end{aligned} \quad (20)$$

The z -distribution is plotted in Fig. 3 for different values of the top polarisation P and the anomalous coupling f_{2R} . One can easily observe that the effect of the anomalous coupling f_{2R} is to change the slope of the z -distribution, which will be explained below.

Since the distribution is linear in z , an analytical expression for the asymmetry can easily be found. We take as the reference point z_c , the value of z which corresponds to $\cos \theta_{b,0} = 0$ i.e. $z_c = (\xi - 1)/2\xi$. To simplify the notation let us define two functions of f_{2R} : $U = f_{1L}^2(\xi + 2) + 6\sqrt{\xi} f_{1L} \text{Re}(f_{2R}) + |f_{2R}|^2(2\xi + 1)$ and $V = -f_{1L}^2(\xi - 2) + 2\sqrt{\xi} f_{1L} \text{Re}(f_{2R}) + |f_{2R}|^2(2\xi - 1)$. Then the distribution in



the z -distribution for different values of f_{2R} . The solid, dashed and dash-dotted lines correspond to $f_{2R} = 0.0, 0.2, -0.2$, respectively

z can be rewritten in terms of $t_{b,0} = \cos \theta_{b,0}$ (see [61, 125]):

$$\frac{1}{\Gamma} \frac{d\Gamma}{dz} = \frac{1}{X} \left(\frac{2\xi(\xi-1)}{\beta} \right) \left[\frac{U}{2} + \frac{PV}{2} t_{b,0} \right]. \quad (21)$$

Now changing the variable from z to $t_{b,0}$ we get the limits of the integration in Eq. 7 as $t_{b,0,\min} = -1$ and $t_{b,0,\max} = 1$. Only the term linear in $t_{b,0}$ survives in the numerator and the expression for A_z is given by

$$A_z = -P \frac{(\xi-1)^2 V}{2X}. \quad (22)$$

Therefore the asymmetry A_z is directly proportional to the top-quark polarisation P and is independent of the boost factor β as V and X are independent of both P and β . Moreover, the z -distribution can be directly related to the angular distribution of the b quark in the top rest frame due to Eq. 19. In fact, substituting the relation Eq. 19 in Eq. 21, we get

$$\frac{1}{\Gamma} \frac{d\Gamma}{d \cos \theta_{b,0}} = \frac{1}{2} [1 + P\alpha \cos \theta_{b,0}] \quad (23)$$

where α is the spin-analysing power of the b quark in the presence of anomalous Wtb coupling f_{2R} . It includes a correction to the SM tree-level value of α_b . To second order in f_{2R} , α can be written as

$$\alpha = - \left(\frac{\xi-2}{\xi+2} \right) + \text{Re}(f_{2R}) \left(\frac{8\sqrt{\xi}(\xi-1)}{(\xi+2)^2} \right) + |f_{2R}|^2 \left(\frac{4(\xi-1)(\xi^2-9\xi+2)}{(\xi+2)^3} \right). \quad (24)$$

Substituting the values of $m_t = 173.5 \text{ GeV}/c^2$ and $m_W = 80.385 \text{ GeV}/c^2$ [1], we get the numerical value of α as

$$\alpha = -0.399 + 1.425 \text{Re}(f_{2R}) - 0.903 |f_{2R}|^2.$$

Since the coefficients of f_{2R} and f_{2R}^2 are much greater than the constant term in the above equation and the alternate terms differ in their signs, cancellation between different terms can occur. Therefore the effect of the anomalous coupling f_{2R} on the z -distribution is non-trivial. As an observable based on the ratio of the energy of the top quark decay products (in the lab frame), A_z can be used along with A_u to probe the top-quark polarisation at large boosts.

3.7 CP violation in the top decay

Here we note that using the asymmetries constructed for the t and \bar{t} decay, one can probe CP violation in the decay of top and anti-top assuming CP conservation in the production of top and anti-top quarks. As mentioned earlier, in the presence of CP conservation $f_{1L} = \bar{f}_{1L}$, $f_{1R} = \bar{f}_{1R}$, $f_{2L} = \bar{f}_{2R}$ and $f_{2R} = \bar{f}_{2L}$. When the production process is CP-conserving, polarisations of the top (P) and the anti-top (\bar{P}) are related: $\bar{P} = -P$. In this limit, the difference

in the u -asymmetries of the top and the anti-top decay is proportional to $\text{Re}(f_{2R}) - \text{Re}(\bar{f}_{2L})$ to linear order in the anomalous couplings (see Eq. 16). The coefficient of proportionality is a function of the top polarisation (P) and the boost β . Here \bar{f}_{1L} is set to unity and \bar{f}_{1R} and \bar{f}_{2R} to zero. Similarly, the difference in z -asymmetries of the top and the anti-top is proportional to $\text{Re}(f_{2R}) - \text{Re}(\bar{f}_{2L})$ with a factor $-4P\sqrt{\xi}(\xi-1)/(\xi+2)^2$ for $\bar{f}_{1L} = 1$ and $\bar{f}_{2R} = 0 = \bar{f}_{1R}$. Note that CP violation in decay necessarily requires an absorptive part in the amplitude and hence in any underlying theory it is expected that $\text{Re}(f_{2R}) - \text{Re}(\bar{f}_{2L})$ would be loop suppressed.

3.8 Sensitivity of the asymmetries to P and f_{2R}

The dependences of various asymmetries on the polarisation of the top quark are compared in Fig. 4. One can observe that for moderate values of the boost $\beta \sim 0.5$ all the four asymmetries are sensitive to the top polarisation, while for large values of boost, A_u and A_z are more sensitive as compared to A_{x_ℓ} and A_{θ_ℓ} . For very small values of boosts ($\beta \approx 0$), the angular asymmetry A_{θ_ℓ} has the highest sensitivity to the top-quark polarisation (P) due the fact that the charged lepton has the maximal spin-analysing power. A_z follows A_{θ_ℓ} in the sensitivity to P for $\beta \approx 0$, as it is directly proportional to the spin-analysing power of the b quark (α). This is true as long as the value of the anomalous coupling f_{2R} does not reduce the value of $|\alpha|$. From Eq. 24 or from the plots of A_z in Fig. 5, one can easily see that the value of α monotonically increases with f_{2R} in the range $[-0.2, 0.2]$. Therefore as a measure of top-quark polarisation, A_z is better for negative values of f_{2R} than for positive values. In a detailed comparison, for $\beta \approx 0$, A_z turns out to be the second best in the sensitivity to P , surpassed only by A_{θ_ℓ} .

An additional result of the comparison is that the sensitivity of A_u to P is higher than that of A_{x_ℓ} in general (see Fig. 4).

Regarding the sensitivity of the asymmetries to f_{2R} , an interesting interplay of the top-quark polarisation and the anomalous coupling f_{2R} can be seen from Fig. 5. For large boost values ($\beta \sim 1$) A_{θ_ℓ} and A_{x_ℓ} have similar sensitivities to f_{2R} (for small values of f_{2R}) which is clearly shown in Fig. 5. In the case of A_z , a nonzero polarisation of the top quark (P) is necessary to probe the anomalous coupling f_{2R} since the asymmetry is directly proportional to P (Sect. 3.3). Moreover A_z is independent of β as mentioned above (Sect. 3.6). This makes A_z a suitable probe of f_{2R} for all values of beta as long as $P \neq 0$. When $P = 0$, A_u and A_{x_ℓ} can be used to measure f_{2R} although the sensitivity of A_{x_ℓ} to f_{2R} (for small f_{2R}) is low at large values of boosts (Fig. 5). The angular asymmetry is not suitable to measure f_{2R} (as long as f_{2R} is small) for any value of the boost as the spin-analysing power α_ℓ is insensitive to f_{2R} (Sect. 3.3). From Fig. 5 one

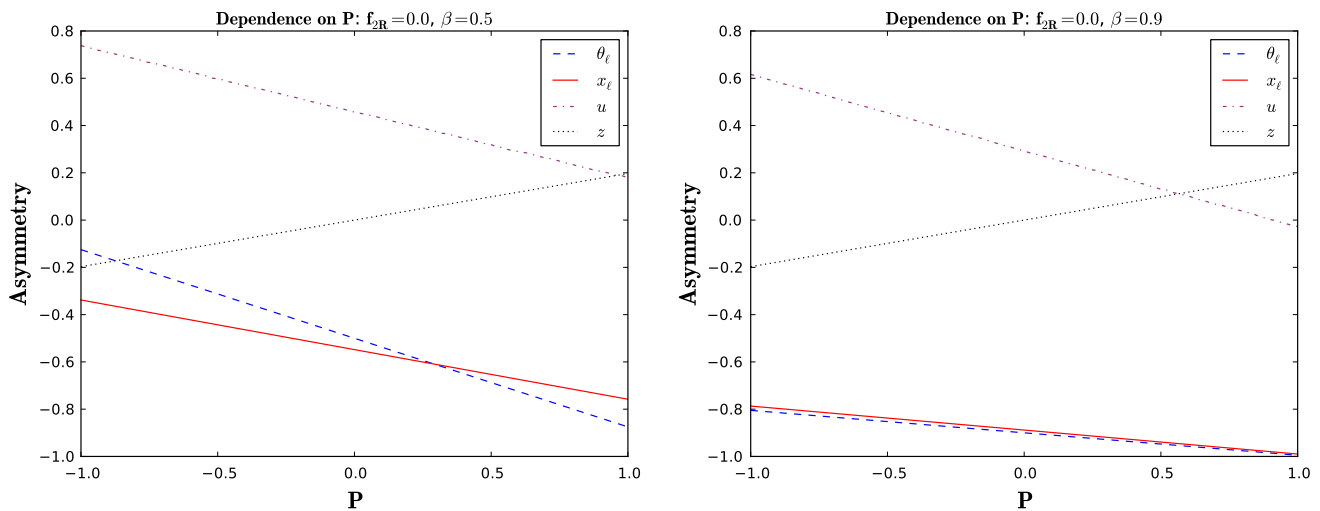


Fig. 4 Comparison of asymmetries in their dependence on the polarisation of the top quark (P) in the lab frame. The boost factors are $\beta = 0.5$ (left) and $\beta = 0.9$ (right), respectively

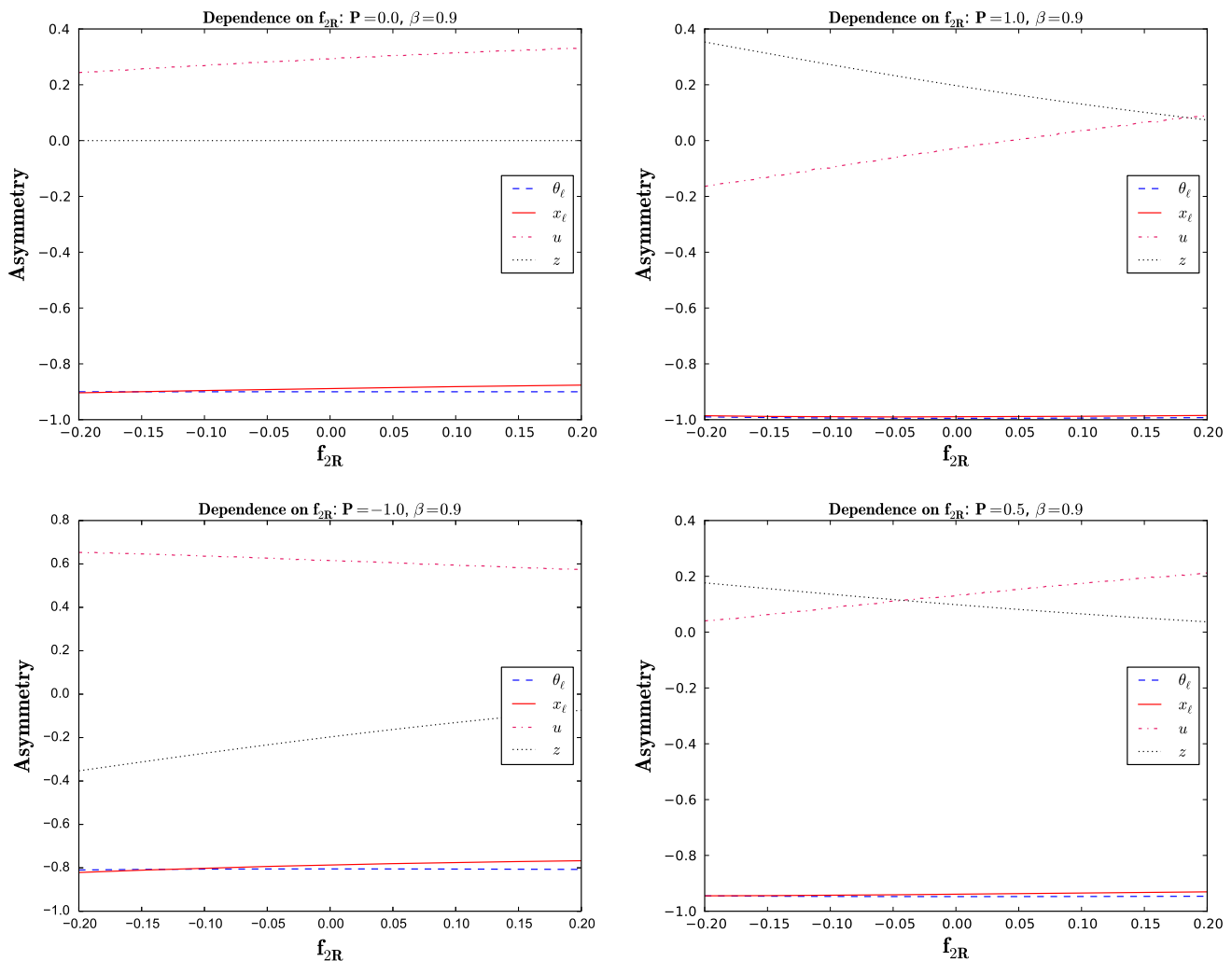


Fig. 5 Comparison of the f_{2R} dependence of various asymmetries for different values of P and f_{2R} for a boost factor $\beta = 0.9$. In each plot the u asymmetry is given in dot-dashed lines, the x_ℓ asymmetry in solid

lines, the θ_ℓ asymmetry in dashed lines and the z asymmetry in dotted lines respectively

can say that for large boosts, A_u can be used to measure f_{2R} irrespective of the top-quark polarisation P . Therefore A_u is the only observable that can be used to measure f_{2R} at large boosts, for any production mechanism of the top quark. However, note that a comparison of the asymmetries for their sensitivities to both the polarisation P and the anomalous coupling f_{2R} , in a realistic experimental set up, requires a careful study of various detector effects on the measurement of asymmetries and is beyond the scope of the present work (see, for example [138]).

4 Constraining P and f_{2R} simultaneously

When $f_{2R} \neq 0$ in the Wtb vertex, the asymmetries considered above are affected by the anomalous coupling f_{2R} along with the polarisation P of the top. Therefore with the measurement of an asymmetry one constrains a region in the two-dimensional P – f_{2R} plane. In this section we compare the asymmetries based on the region each one constrains in the P – f_{2R} plane assuming a plausible set of values of asymmetries expected to be measured at the LHC. We also discuss combining these asymmetries in a χ^2 -based analysis.

4.1 Method of analysis

We assume that the statistical error associated with the measurement of an asymmetry A is given by

$$\Delta A = \frac{1}{\sqrt{N}} \sqrt{1 - A^2} \quad (25)$$

where N is the number of top quarks in the sample of measurement. Given the fact that experimentally measured observables have also systematic uncertainties coming from various sources such as missing higher order corrections to the theoretical predictions, uncertainties in the parton distribution functions, we need to include in ΔA an estimate of the systematic uncertainties associated with the asymmetry A . The total uncertainty on A after including both the statistical and the systematic uncertainties is given by

$$\Delta A = \sqrt{\frac{(1 - A^2)}{N} + \frac{\epsilon^2}{2}(1 - A^2)^2} \quad (26)$$

where ϵ is the fractional systematic uncertainty in the top production cross section at the LHC at $\sqrt{s} = 7$ TeV. The number N appearing in the equations above is estimated from the expected number of top quarks produced at the LHC from heavy resonances with invariant masses of $O(\text{TeV})$ decaying into a top pair. Based on the estimated differential cross section for top-pair production calculated in QCD [139] for the LHC at $\sqrt{s} = 7$ TeV in the invariant-mass window of 1.0 TeV and 1.2 TeV, we take the number of top quarks as

$N = 1.47 \times 10^4$ for an integrated luminosity of 100 fb^{-1} . This number is obtained under the assumption that the top quark decays semileptonically $t \rightarrow b\bar{\ell}\nu$ with $\ell = e, \mu$ and the anti-top decays hadronically. Theoretically an asymmetry is a function of P and f_{2R} and the factor β is close to unity as we consider only those top quarks which are highly boosted in the lab frame. In fact, the boost values of the top quarks produced in the above-mentioned invariant-mass window are in the range 0.94–0.96. As we intend to keep our analysis a qualitative one, we fix β to 0.9.

Suppose that an experimental measurement of A corresponds to a true value (P_0, f_{2R0}) of the parameters P and f_{2R} . This measurement corresponds to an unknown point (P_0, f_{2R0}) in the P – f_{2R} plane. We define a region of significance f around the point (P_0, f_{2R0}) as the region where the value of the asymmetry $A(P, f_{2R})$ is indistinguishable from the experimental value A_{exp} to within f times the error in the measurement ΔA . In other words,

$$\frac{|A_{\text{exp}} - A(P, f_{2R})|}{\Delta A_{\text{exp}}} \leq f. \quad (27)$$

Since our purpose in this paper is to demonstrate the use of asymmetries, we choose a value for P_0 and f_{2R0} ; evaluate ΔA_{exp} using Eq. 25 keeping only the statistical uncertainties and A from the expressions of the corresponding distributions derived in the previous section. The results are shown in Fig. 6.

4.2 χ^2 analysis

We combine three of the four asymmetries to make a χ^2 statistic. One could combine all the four asymmetries to form a χ^2 statistic. We have not considered such a combination in our analysis. This is because we consider, in our analysis, the case of highly boosted top quarks where effectively only the two asymmetries A_u and A_z are sensitive to both P and f_{2R} . Moreover, in the case of $P_0 = 0.0$ and $f_{2R0} = 0.0$, one can easily see from Fig. 6 that the asymmetries A_{θ_ℓ} and A_z are similar in their ability to constrain f_{2R} . Similarly, in the case of $P_0 = -1.0$ and $f_{2R0} = 0.0$, the bounds on f_{2R} are primarily due to A_z and A_u , which can be seen from Fig. 6. The asymmetries A_{θ_ℓ} and A_{x_ℓ} are relatively poor in constraining f_{2R} . In both cases one of A_{x_ℓ} and A_{θ_ℓ} is sufficient to constrain P (see Fig. 6). Hence the inclusion all the four asymmetries at a time in the χ^2 analysis does not improve the best bounds obtained in the current analysis.

There are four ways in which three of the asymmetries A_{x_ℓ} , A_{θ_ℓ} , A_u , A_z can be combined. We discuss each of the combinations. We assume that the asymmetries are measured independently and their errors are given according to either Eq. 26 or Eq. 25 depending on whether the systematic uncer-

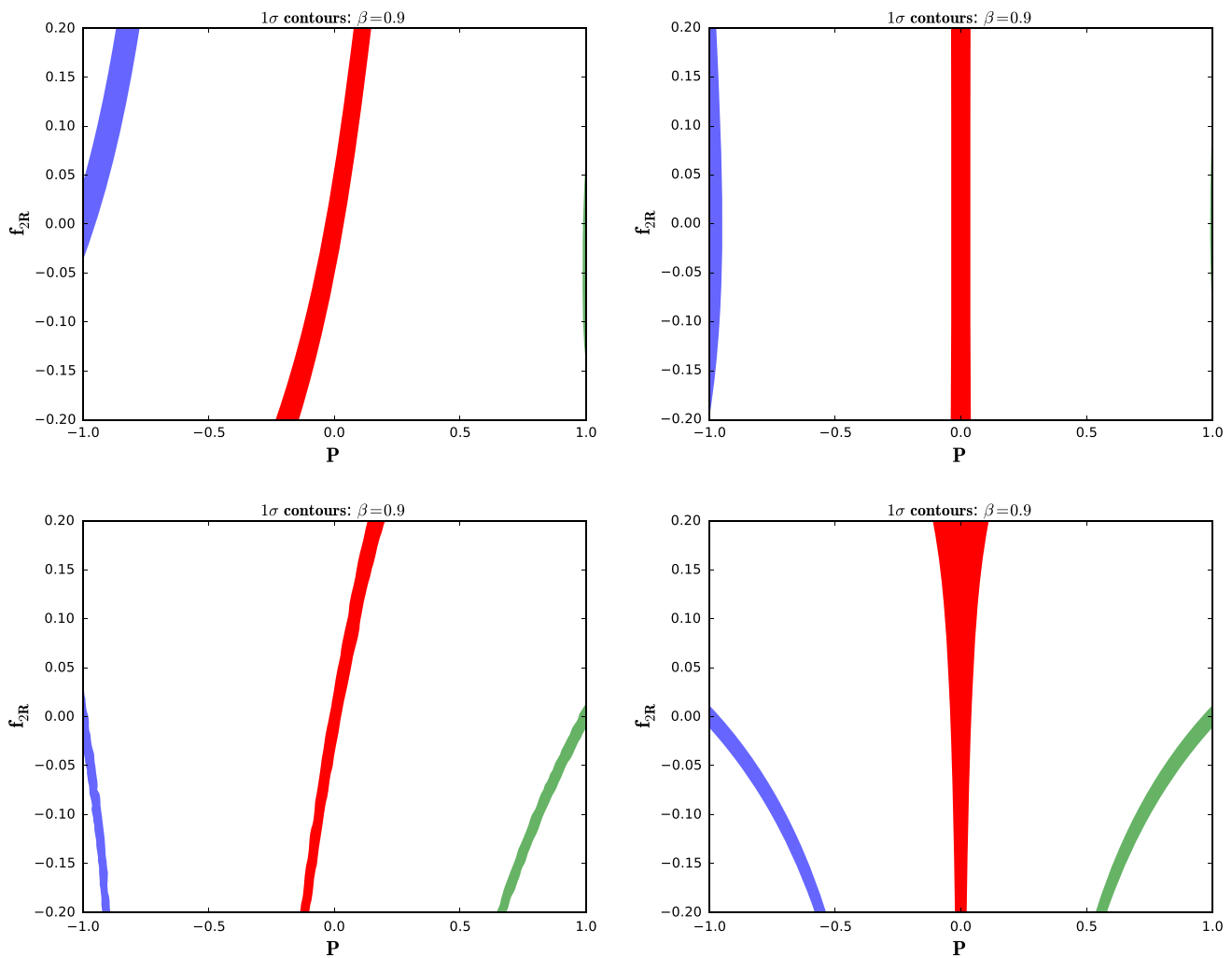


Fig. 6 Comparison of regions with significance less than or equal to 1 for different asymmetries defined in the lab frame: A_{x_ℓ} (upper left), A_{θ_ℓ} (upper right), A_u (bottom left) and A_z (bottom right). The regions shaded in blue (very light), red (dark), green (light) correspond to the

“true” values $P_0 = -1.0$, $f_{2R0} = 0.0$, $P_0 = 0.0$, $f_{2R0} = 0.0$ and $P_0 = 1.0$, $f_{2R0} = 0.0$, respectively. The boost factor β is set to 0.9. In these figures only statistical uncertainties are assumed for the asymmetries

tainties are included or not. The χ^2 is defined by

$$\chi^2 = \sum_i \left(\frac{A_{\text{exp},i} - A_i(P, f_{2R})}{\Delta A_{\text{exp},i}} \right)^2 \quad (28)$$

where $i = x_\ell, \theta_\ell, u, z$.

Since our purpose is to demonstrate the utility of combining asymmetries, we calculate A_{exp} for a “true” value of P and f_{2R} i.e. P_0 and f_{2R0} and evaluate ΔA_{exp} for two cases. In the first case only statistical uncertainties are included in ΔA_{exp} using Eq. 25. In the second case the systematic uncertainties are also included in ΔA_{exp} as given in Eq. 26.

We give contours of $\Delta\chi^2$ values 2.30 and 5.99 corresponding to 68.3 and 95 % C.L (for 2 degrees of freedom), respectively, for both cases. As in the previous section we set $\beta = 0.9$ and use the same number of events N .

Figure 7 shows the $\Delta\chi^2$ contours for four different combinations of asymmetries for $\beta = 0.9$ keeping only the statistical uncertainties. The effects of including systematic uncertainties of the asymmetries in the χ^2 analysis are given later in the text. Table 1 gives the upper bound obtained on P when $f_{2R} = 0.0$, for different combinations of asymmetries, for $\beta = 0.9$. When the true value of P and f_{2R} are $P_0 = 0$, $f_{2R0} = 0$ the combination of A_{θ_ℓ} , A_u and A_z and A_{x_ℓ} , A_u , A_{θ_ℓ} are better in constraining both P and f_{2R} than the other two combinations.

4.3 Limits on f_{2R}

In Tables 2 and 3 we summarise the limits obtained on the anomalous coupling f_{2R} for two values of polarisation $P = 0$ and $P = -1.0$ keeping only statistical uncertainties. The

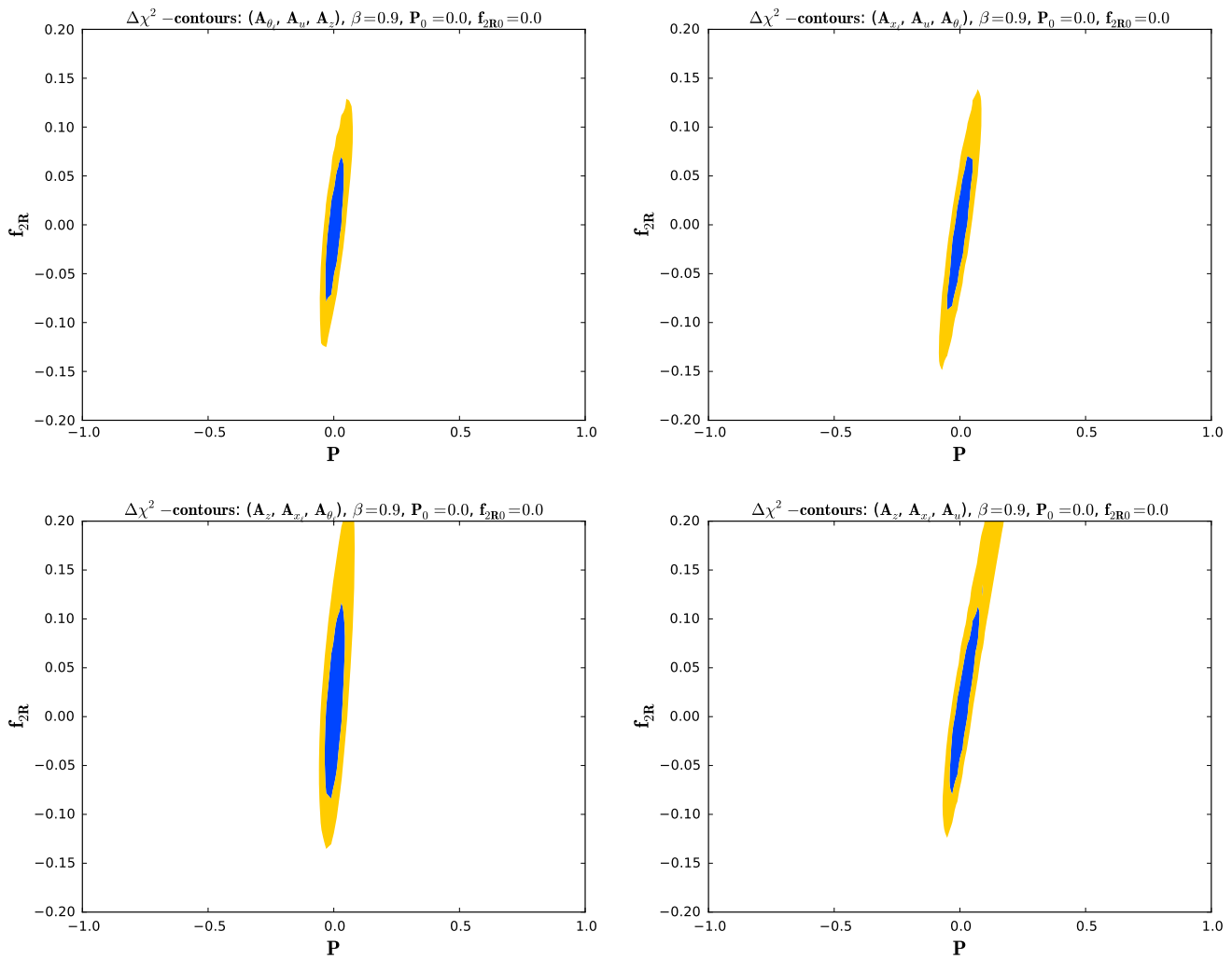


Fig. 7 Contours of $\Delta\chi^2$ corresponding to 68.27 % (blue/darker) and 95 % C.L. (yellow/lighter), respectively, for four combinations of asymmetries: $A_{\theta_\ell}, A_u, A_z$ (top left), $A_{x_\ell}, A_u, A_{\theta_\ell}$ (top right), $A_z, A_{x_\ell}, A_{\theta_\ell}$ (bottom left) and A_z, A_{x_ℓ}, A_u (bottom right). The boost factor is set to

$\beta = 0.9$. The “true” values of P and f_{2R} are $P_0 = 0.0$ and $f_{2R0} = 0.0$, respectively. These contours are for the case where only statistical uncertainties are assumed for the asymmetries

Table 1 The upper limits on the polarisation of the top (P) corresponding to $f_{2R} = 0$ from a $\Delta\chi^2$ analysis. The true values of the parameters are $P_0 = -1.0$ and $f_{2R0} = 0.0$. The lower limit on P is the physical boundary $P = -1.0$. Only statistical uncertainties are assumed for the asymmetries

Combination	1σ	2σ
$A_z, A_{x_\ell}, A_{\theta_\ell}$	−0.96	−0.94
A_z, A_u, A_{x_ℓ}	−0.98	−0.96
$A_{x_\ell}, A_u, A_{\theta_\ell}$	−0.98	−0.96
$A_{\theta_\ell}, A_u, A_z$	−0.97	−0.95

best 1σ limits on f_{2R} obtained in our analysis assuming the top polarisation to be zero is $[-0.079, 0.069]$. The sensitivity increases considerably if, for example, the expected

Table 2 Limits on f_{2R} at 1σ and 2σ level corresponding to the polarisation $P = 0$. Only statistical uncertainties are assumed for the asymmetries

Combination	1σ	2σ
$(A_{\theta_\ell}, A_u, A_z)$	$[-0.079, 0.069]$	$[-0.125, 0.129]$
$(A_{x_\ell}, A_u, A_{\theta_\ell})$	$[-0.087, 0.07]$	$[-0.149, 0.138]$
$(A_z, A_{x_\ell}, A_{\theta_\ell})$	$[-0.083, 0.116]$	$[-0.135, 0.2]$
(A_z, A_{x_ℓ}, A_u)	$[-0.079, 0.112]$	$[-0.124, 0.2]$

polarisation of the top would be -1.0 . The corresponding limit on f_{2R} is $[-0.017, 0.006]$. Now we discuss the results after including systematic uncertainties of asymmetries using Eq. 26 in Eq. 28. The main effect of such an inclusion is that the limits on f_{2R} and P become weaker after the inclusion

Table 3 Limits on f_{2R} at 1σ and 2σ level corresponding to the polarisation $P = -1.0$. Only statistical uncertainties are assumed for the asymmetries

Combination	1σ	2σ
$(A_{\theta_\ell}, A_u, A_z)$	$[-0.017, 0.013]$	$[-0.027, 0.024]$
$(A_{x_\ell}, A_u, A_{\theta_\ell})$	$[-0.039, 0.012]$	$[-0.064, 0.059]$
$(A_z, A_{x_\ell}, A_{\theta_\ell})$	$[-0.019, 0.016]$	$[-0.031, 0.027]$
(A_z, A_{x_ℓ}, A_u)	$[-0.017, 0.006]$	$[-0.029, 0.018]$

of systematic uncertainties. In particular, for $\epsilon \gtrsim 1\%$ the χ^2 statistic does not constrain f_{2R} to between $[-0.2, 0.2]$ in the case of $P_0 = 0.0$. In this case, one may need to use methods such as multivariate analysis, fit to the shape of the distribu-

tions, etc. to constrain P and f_{2R} simultaneously. However, for large values of P_0 our observables are still sensitive to both P and f_{2R} for values of ϵ up to 5 % as can be seen from Fig. 8. A detailed analysis to estimate the systematic uncertainty on the asymmetries would take into account the effects of hadronisation, finite detector resolution etc. on the measurement of asymmetries. Such an analysis would be very useful in improving the bounds on P_0 and f_{2R} compared to our simplified approach and is in progress.

Note that we have analysed the case of $t\bar{t}$ pair production using events with $t\bar{t}$ invariant masses in the range 1.0 TeV to 1.2 TeV so as to analyse $t\bar{t}$ pairs possibly coming from a resonance. Even with an integrated luminosity of 100 fb^{-1} at $\sqrt{s} = 7 \text{ TeV}$ LHC, the number of top events in this analysis is considerably lower than the number used in the analyses

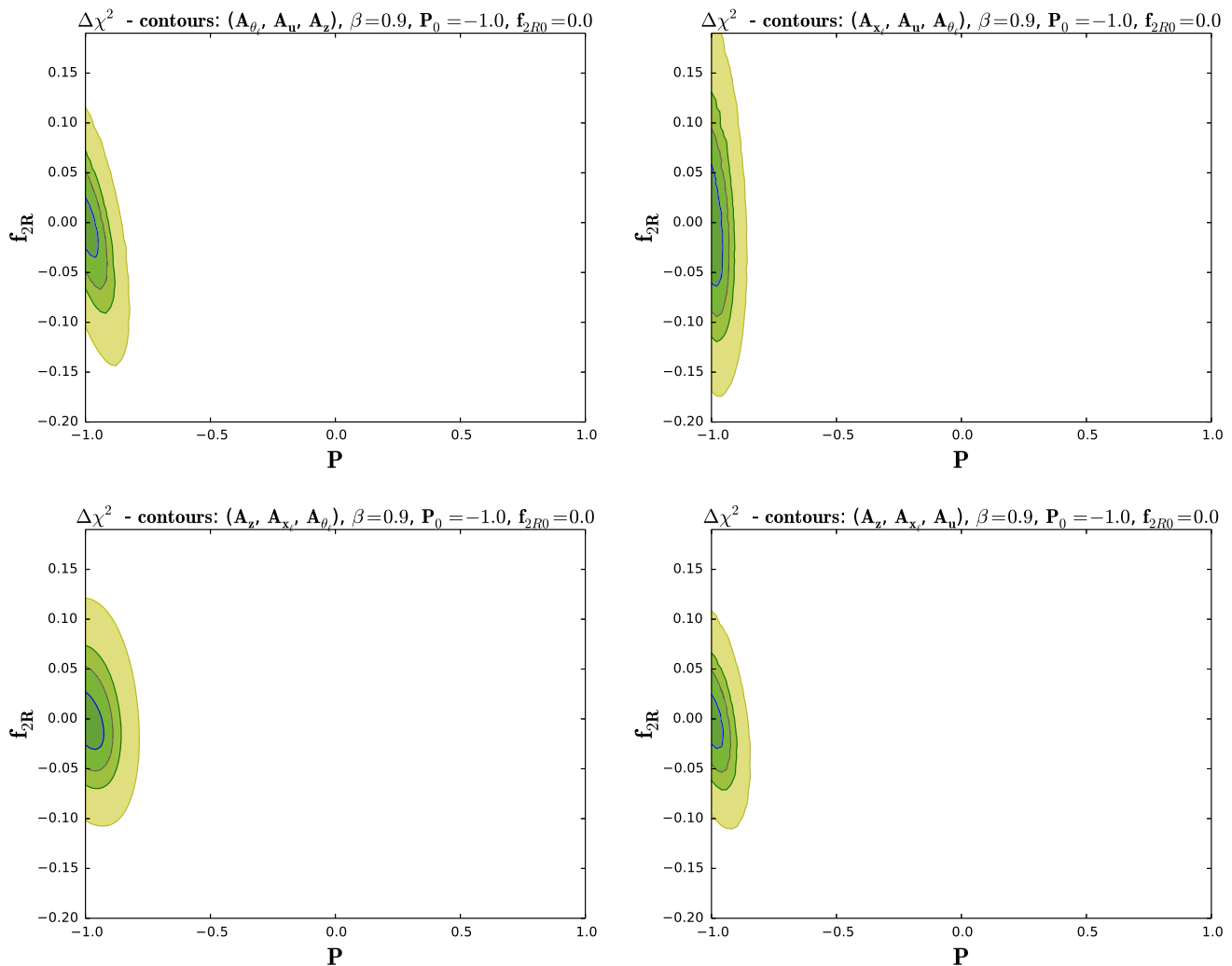


Fig. 8 Contours of $\Delta\chi^2$ corresponding to 95 % C.L are given for four values of the systematic uncertainty parameter ϵ for each of the four combinations of asymmetries: $A_{\theta_\ell}, A_u, A_z$ (top left), $A_{x_\ell}, A_u, A_{\theta_\ell}$ (top right), $A_z, A_{x_\ell}, A_{\theta_\ell}$ (bottom left) and A_z, A_{x_ℓ}, A_u (bottom right). The systematic uncertainties associated with the asymmetries are calculated

according to Eq. 26. In each figure, the darker to lighter contours correspond to $\epsilon = 0.0, 0.02, 0.03, 0.05$, respectively. The boost factor is set to $\beta = 0.9$. The “true” values of P and f_{2R} are $P_0 = -1.0$ and $f_{2R0} = 0.0$ respectively

such as [117], which uses $t\bar{t}$ events over the entire range of the invariant mass. Due to the lower statistics our limits on f_{2R} for the case of zero polarisation are weaker than the limits obtained in [117]. But they are compatible with the CMS measurement of f_{2R} : $0.07 \pm 0.053(\text{stat})_{-0.073}^{+0.081}(\text{syst})$ using 2.2 fb^{-1} of integrated luminosity at $\sqrt{s} = 7 \text{ TeV}$. Note that our results are compatible with the result obtained by the CMS experiment with 2.2 fb^{-1} luminosity (corresponding to a number of events $N \sim O(10^4)$) and hence a smaller number of $t\bar{t}$ events than the ATLAS analysis, using the $t\bar{t}$ events with invariant masses over the whole allowed range. This gives us confidence that the various limits indicated in this report are representative of what can be achieved in a real analysis. However, with this luminosity the observables are not sensitive to the contribution of the SM higher order corrections to the anomalous couplings, including f_{2R} . This is because their values are very small (see Sect. 2) compared to the size of the bounds obtained in our analysis, which are of the order of 10^{-2} – 10^{-1} .

5 Summary

In this work we have taken up the study of observables constructed out of kinematical variables of top decay products for the purpose of measuring the top polarisation in the presence of anomalous Wtb couplings as well as measuring the anomalous coupling f_{2R} itself. We concentrate on laboratory-frame variables which do not require the reconstruction of the top rest frame. An important consideration has been the degree of the boost of the decaying top, since for many practical processes, as, for example, a heavy resonance decaying into a top pair, the top quark is produced with large momentum in the lab frame.

We have considered four observables; asymmetries in the variables θ_ℓ , u , x_ℓ and z . They are compared for their sensitivities to the polarisation of the top quark and the anomalous coupling f_{2R} . We state the results of the comparison of asymmetries in two categories: (1) asymmetries for the measurement of the top-quark polarisation P , and (2) asymmetries for the measurement of the anomalous coupling f_{2R} .

As for the first category of asymmetries for the measurement of the top-quark polarisation, for small values of boost from the top quark rest frame to the lab frame ($\beta \approx 0$), A_{θ_ℓ} is the most sensitive observable. Next in sensitivity is A_z as long as f_{2R} is small or negative. For large values of boosts ($\beta \sim 1$), A_u and A_z can be used as they are much more sensitive to P compared to A_{x_ℓ} and A_{θ_ℓ} .

For the second category corresponding to the measurement of the anomalous coupling f_{2R} , for all values of β , A_z can be used to measure f_{2R} as long as $P \neq 0$. For $P = 0$, A_u , A_z can be used to measure f_{2R} for any β . The angular asymmetry A_{θ_ℓ} is not suitable as a measure of f_{2R} for any

value of β as its sensitivity to f_{2R} is much more smaller than the sensitivities of A_u and A_z . Irrespective of the production mechanism of the top quark, A_u can be used to measure f_{2R} at large values of the boost β .

In all cases, we determine the 1σ and 2σ limits that the measurement of asymmetries can put on the determination of the polarisation or f_{2R} with a chosen number of events. We also do an analysis of the use of combination of asymmetries for the simultaneous determination of the top polarisation as well as f_{2R} . Finally we study the effects of including systematic uncertainties of asymmetries and find that for large values of the top polarisation our observables are sensitive to both P and f_{2R} for systematic uncertainties up to $\sim 5\%$.

Note added While our manuscript was in preparation a related work [140] appeared. In this work, correlations of the anomalous couplings $f_{1L,R}$ and $f_{2L,R}$ are obtained through global fits to data on observables that are insensitive to the polarisation of the top. The authors of the reference point out the need of measuring the single top cross section to 1 % precision as this would put strong constraints on the new physics that affects the Wtb vertex. However, our method, which uses observables sensitive to top polarisation, when used for processes such as single top production and decay, is sensitive to new physics even when the cross section is measured only to 5 %.

Acknowledgments RMG wishes to acknowledge support from the Department of Science and Technology, India, under Grant No. SR/S2/JCB-64/2007. SDR acknowledges support from the Department of Science and Technology, India, under the J.C. Bose National Fellowship programme, Grant No. SR/SB/JCB-42/2009.

Open Access This article is distributed under the terms of the Creative Commons Attribution 4.0 International License (<http://creativecommons.org/licenses/by/4.0/>), which permits unrestricted use, distribution, and reproduction in any medium, provided you give appropriate credit to the original author(s) and the source, provide a link to the Creative Commons license, and indicate if changes were made. Funded by SCOAP³.

Appendix A: The x_ℓ -distribution

The differential distribution $(1/\Gamma)d^2\Gamma/dx_{\ell,0}d\cos\theta_{\ell,0}$ defined in the top quark rest frame is given by

$$\begin{aligned} \frac{1}{\Gamma} \frac{d^2\Gamma}{dx_{\ell,0}d\cos\theta_{\ell,0}} = & \frac{3\xi^2}{X} (1 - x_{\ell,0}) \left[f_{1L}^2 \xi x_{\ell,0} (1 + P t_0) \right. \\ & + 2 f_{1L} \text{Re}(f_{2R}) \sqrt{\xi} (1 + P t_0) \\ & + |f_{2R}|^2 \left\{ P t_0 \left(\xi x_{\ell,0} + \frac{2}{x_{\ell,0}} - (\xi + 1) \right) \right. \\ & \left. \left. + (\xi + 1) - x_{\ell,0} \xi \right\} \right] \end{aligned} \quad (\text{A.1})$$

where $t_0 = \cos \theta_{\ell,0}$ the cosine of the angle between the top spin direction and the lepton momentum and X is as defined in Eq. 10³. It is also the polar angle of the lepton due to our choice of the top rest frame (see footnote in Sect. 1). In the above equation, the top polarisation points in the direction of motion of the top. When the top polarisation points in a general direction in the top rest frame, the differential distribution of the top decay is given, to linear order in f_{2R} by

$$\begin{aligned} & \frac{1}{\Gamma} \frac{d\Gamma}{dx_{\ell,0} dt_0 d\phi_0 d\alpha_0} \\ &= \frac{3\xi^2}{X} \frac{1}{(2\pi)^2} (1 - x_{\ell,0}) \left\{ f_{1L}^2 \xi x_{\ell,0} (1 + \vec{P} \cdot \hat{p}_{\ell,0}) \right. \\ &+ 2\sqrt{\xi} \text{Re}(f_{1L} f_{2R}^*) \left[\xi x_{\ell,0} (1 + \vec{P} \cdot \hat{p}_{\ell,0}) \right. \\ &+ (1 - \xi x_{\ell}) + \frac{1}{2} x_{\ell} (\xi - 1) \vec{P} \cdot (\hat{p}_{b,0} - \hat{p}_{\ell,0}) \left. \right] \\ &\left. - \sqrt{\xi} \text{Im}(f_{1L} f_{2R}^*) x_{\ell,0} (\xi - 1) \vec{P} \cdot (\hat{p}_{b,0} \times \hat{p}_{\ell,0}) \right\} \quad (\text{A.2}) \end{aligned}$$

where $\hat{p}_{\ell,0}$ and $\hat{p}_{b,0}$ are the unit vectors along the direction of momenta of the lepton and the b -quark in the top rest frame, respectively; $\phi_{\ell,0}$ and α_0 are the azimuthal angles of the lepton and the b -quark as mentioned in Sect. 3.5.

Now we consider lab frame distributions. Let β be the magnitude of the boost required to go from the top rest frame to the lab frame. The corresponding Lorentz transformation relates the energy and the polar angle of the lepton measured in these two frames by

$$\begin{aligned} x_{\ell} &= \gamma(x_{\ell,0} + \beta x_{\ell,0} \cos \theta_{\ell,0}) = \gamma x_{\ell,0} (1 + \beta t_0), \\ x_{\ell} \cos \theta_{\ell} &= \gamma(x_{\ell,0} \cos \theta_{\ell,0} + \beta x_{\ell,0}) = \gamma x_{\ell,0} (t_0 + \beta). \end{aligned} \quad (\text{A.3})$$

The inverse relations are

$$\begin{aligned} x_{\ell,0} &= \gamma(x_{\ell} - \beta x_{\ell} \cos \theta_{\ell}) = \gamma x_{\ell} (1 - \beta t), \\ x_{\ell,0} \cos \theta_{\ell,0} &= \gamma(x_{\ell} \cos \theta_{\ell} - \beta x_{\ell}) = \gamma x_{\ell} (t - \beta). \end{aligned} \quad (\text{A.4})$$

Now the differential distribution $(1/\Gamma) d^2\Gamma/dx_{\ell,0} dt_0$ is transformed to $(1/\Gamma) d^2\Gamma/dx_{\ell} dt$ accordingly. We have

$$\begin{aligned} \frac{1}{\Gamma} \frac{d^2\Gamma}{dx_{\ell} dt} &= \frac{3(1 - \beta^2)\xi^2}{x_{\ell}(1 - \beta t)^3 X} (\gamma x_{\ell} (\beta t - 1) + 1) \\ &\times [f_{1L}^2 \gamma^2 \xi x_{\ell}^2 (\beta t - 1)^2 (P(t - \beta) - \beta t + 1) \\ &- 2\gamma \sqrt{\xi} f_{1L} \text{Re}(f_{2R}) x_{\ell} (\beta t - 1) (P(t - \beta) - \beta t + 1) \end{aligned}$$

³ We verified that upon integration over the azimuthal angles of the b -quark and the lepton all the structures of Eq. (A8) of [33] agree with those of our Eq. A.1. We have also checked that all the structures that appear in Eq. (A8) of [33] are present in intermediate stages of the calculations that lead to Eq. A.1.

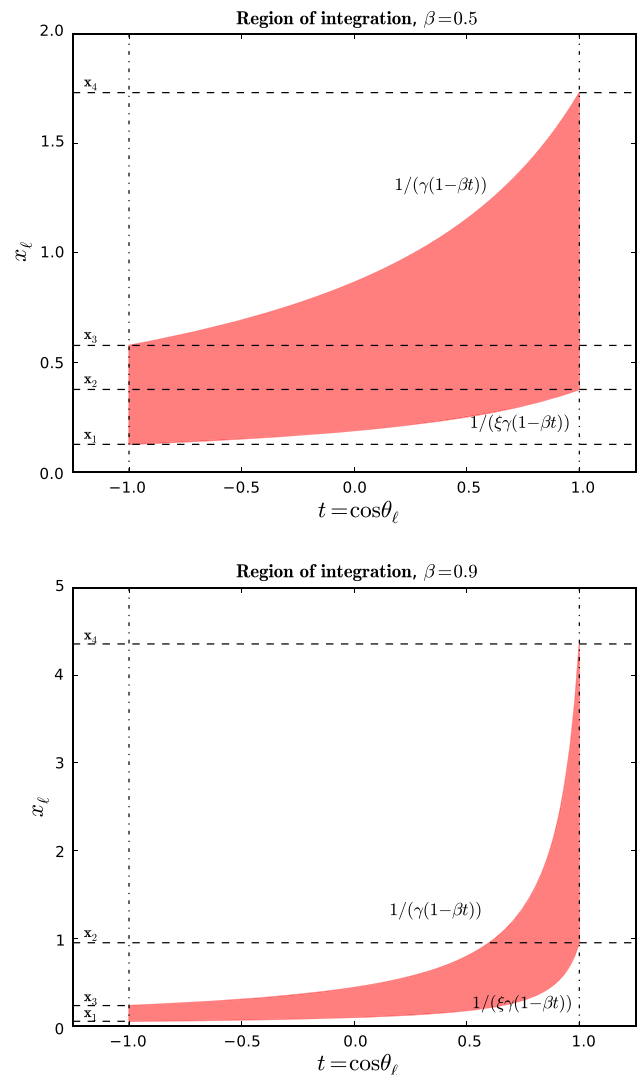


Fig. 9 Regions of integration for the x_{ℓ} distribution. The top (bottom) figure corresponds to $\beta = 0.5$ ($\beta = 0.9$)

$$\begin{aligned} &+ |f_{2R}|^2 (P(t - \beta) (\gamma^2 \xi x_{\ell}^2 (\beta t - 1)^2 \\ &+ \gamma x_{\ell} (\xi + 1) (\beta t - 1) + 2) \\ &+ \gamma x_{\ell} (\beta t - 1)^2 (\xi (\gamma x_{\ell} (\beta t - 1) + 1) + 1))]. \end{aligned} \quad (\text{A.5})$$

Integrating the differential distribution $(1/\Gamma) d^2\Gamma/dx_{\ell} dt$ over $t = \cos \theta_{\ell}$ in the region bounded by Eq. A.4 gives the distribution $(1/\Gamma) d\Gamma/dx_{\ell}$.

The region of integration is given in Fig. 9 for two different values of the boost chosen such that the left (right) figure corresponds to $\beta < \beta_c$ ($\beta > \beta_c$). $\beta_c = (\xi - 1)/(\xi + 1) \approx 0.643$ is the value of the boost where the lowest ordinate of the curve $x = 1/(\gamma(1 - \beta t))$ equals the maximum ordinate of the curve $x = 1/(\xi \gamma(1 - \beta t))$. As shown in Fig. 9 the range of x_{ℓ} is divided into three regions, each having a separate integration limit on t . For $\beta < \beta_c = (\xi -$

$1)/(\xi + 1)$, we have $[x_1, x_2]$, $[x_2, x_3]$, $[x_3, x_4]$ where $x_1 = (1/\xi)\sqrt{(1-\beta)/(1+\beta)}$, $x_2 = (1/\xi)\sqrt{(1+\beta)/(1-\beta)}$, $x_3 = \sqrt{(1-\beta)/(1+\beta)}$, $x_4 = \sqrt{(1+\beta)/(1-\beta)}$, for $\beta > \beta_c$, the range of x_ℓ is divided into $[x_1, x_3]$, $[x_3, x_2]$, $[x_2, x_4]$ and for $\beta = \beta_c$, $x_2 = x_3$. We first consider the case $\beta < \beta_c$. The distribution $(1/\Gamma)d\Gamma/dx_\ell$ is called $R1(x_\ell)$ in the region $[x_1, x_2]$, $R2(x_\ell)$ in the region $[x_2, x_3]$ and $R3(x_\ell)$ in the region $[x_3, x_4]$.

The expressions are given for $f_{2R} = 0$ by

$$R1(x_\ell) = -\frac{3\xi}{2\beta^2(\xi-1)^2(\xi+2)} \left[(P-\beta)(1-2\xi)\sqrt{1-\beta^2} - 2\xi Px_\ell(1-\beta^2) + x_\ell^2\xi^2(P+\beta)\sqrt{1-\beta^2} + 2\beta^2x_\ell^2\xi^2(1-P)\sqrt{\frac{1+\beta}{1-\beta}} + 2x_\ell\xi^2(P-\beta)(1+\beta) - x_\ell\xi^2P(1-\beta^2)\log\left(\frac{1+\beta}{1-\beta}\right) - 2x_\ell\xi^2P(1-\beta^2)\log(x_\ell\xi) \right], \quad (\text{A.6})$$

$$R2(x_\ell) = \frac{6x_\ell\xi^3}{(\xi+2)(\xi-1)^2} \left[1 - \frac{P}{\beta} - \frac{x_\ell}{\sqrt{1-\beta^2}} + \frac{Px_\ell\beta}{\sqrt{1-\beta^2}} + \frac{P(1-\beta^2)}{\beta^2} \tanh^{-1}\beta \right], \quad (\text{A.7})$$

$$R3(x_\ell) = -\frac{3\xi^3}{2\beta^2(\xi-1)^2(\xi+2)} \left[(P-\beta)\sqrt{1-\beta^2} - x_\ell^2 \left((P+\beta)\sqrt{1-\beta^2} - 2\beta^2(1+P)\sqrt{\frac{1-\beta}{1+\beta}} \right) + 2x_\ell(1-\beta) \left(\beta(1+P) + P(1+\beta)\log x_\ell + \frac{1}{2}P(1+\beta)\log\left(\frac{1-\beta}{1+\beta}\right) \right) \right]. \quad (\text{A.8})$$

Similarly for $\beta > \beta_c$, functions corresponding to the intervals $[x_1, x_3]$, $[x_3, x_2]$, $[x_2, x_4]$ are called $S1(x_\ell)$, $S2(x_\ell)$ and $S3(x_\ell)$, respectively. We have $S1(x_\ell) = R1(x_\ell)$ and $S3(x_\ell) = R3(x_\ell)$;

$$S2(x_\ell) = \frac{3\xi\sqrt{1-\beta^2}}{2\beta^2(\xi-1)^2(\xi+2)} \left[(\xi-1)^2(\beta-P) + 2Px_\ell\sqrt{1-\beta^2}(\xi^2\log\xi - \xi(\xi-1)) \right]. \quad (\text{A.9})$$

References

- J. Beringer et al., (Particle Data Group), Phys. Rev. D **86**, 010001 (2012)
- M. Beneke, I. Efthymiopoulos, M.L. Mangano, J. Womersley, A. Ahmadov, et al., (2000). [arXiv:hep-ph/0003033](#) [hep-ph]
- T. Han, Int. J. Mod. Phys. A **23**, 4107 (2008). [arXiv:0804.3178](#) [hep-ph]
- W. Bernreuther, J. Phys. G **35**, 083001 (2008). [arXiv:0805.1333](#) [hep-ph]
- F.-P. Schilling, Int. J. Mod. Phys. A **27**, 1230016 (2012). [arXiv:1206.4484](#) [hep-ex]
- E. Barberis, Int. J. Mod. Phys. A **28**, 1330027 (2013)
- S. Jabeen, Int. J. Mod. Phys. A **28**, 1330038 (2013)
- G. Aad, et al. (ATLAS), Phys. Rev. Lett. **111**, 232002 (2013). [arXiv:1307.6511](#) [hep-ex]
- CMS, W helicity in top pair events. Tech. Rep. CMS-PAS-TOP-11-020, CERN, Geneva (2012)
- K.-M. Cheung, Phys. Rev. D **53**, 3604 (1996). [arXiv:hep-ph/9511260](#) [hep-ph]
- P. Poulose, S.D. Rindani, Phys. Rev. D **54**, 4326 (1996)
- P. Poulose, S.D. Rindani, Phys. Rev. D **61**, 119901 (2000)
- R.M. Godbole, S.D. Rindani, R.K. Singh, Phys. Rev. D **67**, 095009 (2003). [arXiv:hep-ph/0211136](#) [hep-ph]
- D. Choudhury, P. Saha, Pramana **77**, 1079 (2011). [arXiv:0911.5016](#) [hep-ph]
- S.K. Gupta, A.S. Mete, G. Valencia, Phys. Rev. D **80**, 034013 (2009). [arXiv:0905.1074](#) [hep-ph]
- Z. Hioki, K. Ohkuma, Phys. Rev. D **83**, 114045 (2011). [arXiv:1104.1221](#) [hep-ph]
- D. Choudhury, P. Saha, JHEP **1208**, 144 (2012). [arXiv:1201.4130](#) [hep-ph]
- O. Antipin, G. Valencia, Phys. Rev. D **79**, 013013 (2009). [arXiv:0807.1295](#) [hep-ph]
- W. Bernreuther, Z.-G. Si, Phys. Lett. B **725**, 115 (2013). [arXiv:1305.2066](#) [hep-ph]
- B. Buchmuller, D. Wyler, Nucl. Phys. B **268**, 621 (1986)
- B. Grzadkowski, Z. Hioki, K. Ohkuma, J. Wudka B **689**, 108 (2004). [arXiv:hep-ph/0310159](#) [hep-ph]
- B. Grzadkowski, M. Iskrzynski, M. Misiak, J. Rosiek, JHEP **1010**, 085 (2010). [arXiv:1008.4884](#) [hep-ph]
- J. Aguilar-Saavedra, Nucl. Phys. B **812**, 181 (2009). [arXiv:0811.3842](#) [hep-ph]
- F. Bach, T. Ohl, Phys. Rev. D **86**, 114026 (2012). [arXiv:1209.4564](#) [hep-ph]
- C. Zhang, S. Willenbrock, Phys. Rev. D **83**, 034006 (2011). [arXiv:1008.3869](#) [hep-ph]
- M. Fischer, S. Groote, J. Korner, M. Mauser, Phys. Rev. D **65**, 054036 (2002). [arXiv:hep-ph/0101322](#) [hep-ph]
- A. Czarnecki, Phys. Lett. B **252**, 467 (1990)
- C.S. Li, R.J. Oakes, T.C. Yuan, Phys. Rev. D **43**, 3759 (1991)
- G.A. Gonzalez-Sprinberg, R. Martinez, J. Vidal, JHEP **1107**, 094 (2011). [arXiv:1105.5601](#) [hep-ph]
- M. Jezabek, J.H. Kuhn, Nucl. Phys. B **320**, 20 (1989)
- A. Czarnecki, M. Jezabek, J.H. Kuhn, Nucl. Phys. B **351**, 70 (1991)
- G.L. Kane, G.A. Ladinsky, C.P. Yuan, Phys. Rev. D **45**, 124 (1992)
- W. Bernreuther, O. Nachtmann, P. Overmann, T. Schröder, Nucl. Phys. B **388**(1), 53 (1992); Erratum, Nucl. Phys. B **406**, 516 (1993)
- M. Jezabek, J.H. Kuhn, Phys. Lett. B **329**, 317 (1994). [arXiv:hep-ph/9403366](#) [hep-ph]
- C.A. Nelson, B.T. Kress, M. Lopes, T.P. McCauley, Phys. Rev. D **56**, 5928 (1997). [arXiv:hep-ph/9707211](#) [hep-ph]
- R.M. Godbole, S.D. Rindani, R.K. Singh, JHEP **0612**, 021 (2006). [arXiv:hep-ph/0605100](#) [hep-ph]
- S.D. Rindani, Pramana **54**, 791 (2000). [arXiv:hep-ph/0002006](#) [hep-ph]
- M. Jezabek, J.H. Kuhn, Nucl. Phys. B **314**, 1 (1989)
- A. Brandenburg, Z. Si, P. Uwer, Phys. Lett. B **539**, 235 (2002). [arXiv:hep-ph/0205023](#) [hep-ph]

40. W. Bernreuther, M. Fuecker, Y. Umeda, Phys. Lett. B **582**, 32 (2004). [arXiv:hep-ph/0308296](#) [hep-ph]
41. S. Groote, W. Huo, A. Kadeer, J. Korner, Phys. Rev. D **76**, 014012 (2007). [arXiv:hep-ph/0602026](#) [hep-ph]
42. K. Hagiwara, K. Mawatari, H. Yokoya, JHEP **0712**, 041 (2007). [arXiv:0707.3194](#) [hep-ph]
43. Y. Kitadono, H.-n Li, Phys. Rev. D **87**(5), 054017 (2013). [arXiv:1211.3260](#) [hep-ph]
44. M. Brucherseifer, F. Caola, K. Melnikov, JHEP **1304**, 059 (2013). [arXiv:1301.7133](#) [hep-ph]
45. W. Bernreuther, P. Gonzlez, C. Mellein, Eur. Phys. J. C **74**(3), 2815 (2014). [arXiv:1401.5930](#) [hep-ph]
46. W. Bernreuther, M. Fuecker, Z.-G. Si, Phys. Rev. D **74**, 113005 (2006). [arXiv:hep-ph/0610334](#) [hep-ph]
47. W. Bernreuther, M. Fucker, Z.-G. Si, Phys. Rev. D **78**, 017503 (2008). [arXiv:0804.1237](#) [hep-ph]
48. J.H. Kuhn, A. Scharf, P. Uwer, Eur. Phys. J. C **51**, 37 (2007). [arXiv:hep-ph/0610335](#) [hep-ph]
49. J.H. Kühn, A. Scharf, P. Uwer, Phys. Rev. D **91**, 014020 (2015)
50. G. Mahlon, S.J. Parke, Phys. Lett. B **476**, 323 (2000). [arXiv:hep-ph/9912458](#) [hep-ph]
51. R. Schwienhorst, C.-P. Yuan, C. Mueller, Q.-H. Cao, Phys. Rev. D **83**, 034019 (2011). [arXiv:1012.5132](#) [hep-ph]
52. W.G. Dharmaratna, G.R. Goldstein, Phys. Rev. D **41**, 1731 (1990)
53. W. Bernreuther, A. Brandenburg, P. Uwer, Phys. Lett. D **368**, 153 (1996). [arXiv:hep-ph/9510300](#) [hep-ph]
54. M. Baumgart, B. Tweedie, JHEP **1308**, 072 (2013). [arXiv:1303.1200](#) [hep-ph]
55. M.M. Nojiri, Phys. Rev. D **51**, 6281 (1995). [arXiv:hep-ph/9412374](#) [hep-ph]
56. M. Perelstein, A. Weiler, JHEP **0903**, 141 (2009). [arXiv:0811.1024](#) [hep-ph]
57. M. Arai, K. Huitu, S.K. Rai, K. Rao, JHEP **1008**, 082 (2010). [arXiv:1003.4708](#) [hep-ph]
58. S. Gopalakrishna, T. Han, I. Lewis, Z.-g Si, Y.F. Zhou, Phys. Rev. D **82**, 115020 (2010). [arXiv:1008.3508](#) [hep-ph]
59. R.M. Godbole, K. Rao, S.D. Rindani, R.K. Singh, JHEP **1011**, 144 (2010). [arXiv:1010.1458](#) [hep-ph]
60. K. Huitu, S. Kumar Rai, K. Rao, S.D. Rindani, P. Sharma, JHEP **1104**, 026 (2011). [arXiv:1012.0527](#) [hep-ph]
61. S.D. Rindani, P. Sharma **1111**, 082 (2011). [arXiv:1107.2597](#) [hep-ph]
62. S.S. Biswal, S.D. Rindani, P. Sharma, Phys. Rev. D **88**, 074018 (2013). [arXiv:1211.4075](#) [hep-ph]
63. G. Belanger, R. Godbole, L. Hartgring, I. Niessen, JHEP **1305**, 167 (2013). [arXiv:1212.3526](#)
64. G. Belanger, R.M. Godbole, S. Kraml, S. Kulkarni (2013). [arXiv:1304.2987](#) [hep-ph]
65. S. Taghavi, M.M. Najafabadi, Int. J. Theor. Phys. **53**, 4326 (2014). [arXiv:1301.3073](#) [hep-ph]
66. J. Aguilar-Saavedra, S.A. dos Santos, Phys. Rev. D **89**, 114009 (2014). [arXiv:1404.1585](#) [hep-ph]
67. J. Cao, L. Wu, J.M. Yang, Phys. Rev. D **83**, 034024 (2011). [arXiv:1011.5564](#) [hep-ph]
68. D. Choudhury, R.M. Godbole, S.D. Rindani, P. Saha, Phys. Rev. D **84**, 014023 (2011). [arXiv:1012.4750](#) [hep-ph]
69. D. Krohn, T. Liu, J. Shelton, L.-T. Wang, Phys. Rev. D **84**, 074034 (2011). [arXiv:1105.3743](#) [hep-ph]
70. A. Falkowski, G. Perez, M. Schmaltz, Phys. Rev. D **87**, 034041 (2013). [arXiv:1110.3796](#) [hep-ph]
71. R.M. Godbole, L. Hartgring, I. Niessen, C.D. White, JHEP **1201**, 011 (2012). [arXiv:1111.0759](#) [hep-ph]
72. L. Randall, R. Sundrum, Phys. Rev. Lett. **83**, 3370 (1999). [arXiv:hep-ph/9905221](#) [hep-ph]
73. K. Agashe, R. Contino, A. Pomarol, Nucl. Phys. B **719**, 165 (2005). [arXiv:hep-ph/0412089](#) [hep-ph]
74. K. Agashe, A. Belyaev, T. Krupovnickas, G. Perez, J. Virzi, Phys. Rev. D **77**, 015003 (2008). [arXiv:hep-ph/0612015](#) [hep-ph]
75. J. Shelton, Phys. Rev. D **79**, 014032 (2009). [arXiv:0811.0569](#) [hep-ph]
76. D. Krohn, J. Shelton, L.-T. Wang, JHEP **1007**, 041 (2010). [arXiv:0909.3855](#) [hep-ph]
77. B. Bhattacharjee, S.K. Mandal, M. Nojiri **1303**, 105 (2013). [arXiv:1211.7261](#) [hep-ph]
78. Y. Kitadono, H.-N. Li, Phys. Rev. D **89**(11), 114002 (2014). [arXiv:1403.5512](#) [hep-ph]
79. B. Tweedie, Phys. Rev. D **90**, 094010 (2014). [arXiv:1401.3021](#) [hep-ph]
80. S. Chatrchyan et al. (CMS Collaboration), JHEP **1212**, 015 (2012). [arXiv:1209.4397](#) [hep-ex]
81. S. Chatrchyan et al., Phys. Lett. B **720**, 63 (2013). [arXiv:1212.6175](#) [hep-ex]
82. G. Aad et al. (ATLAS Collaboration), Phys. Rev. D **86**, 091103 (2012). [arXiv:1209.6593](#) [hep-ex]
83. G. Aad et al., JHEP **1301**, 116 (2013). [arXiv:1211.2202](#) [hep-ex]
84. G. Aad et al., Phys. Rev. D **88**, 012004 (2013). [arXiv:1305.2756](#) [hep-ex]
85. I. Low, Phys. Rev. D **88**, 095018 (2013). [arXiv:1304.0491](#) [hep-ph]
86. K.-I. Hikasa, J.M. Yang, B.-L. Young, Phys. Rev. D **60**, 114041 (1999). [arXiv:hep-ph/9908231](#) [hep-ph]
87. Y.M. Nie, C.S. Li, Q. Li, J.J. Liu, J. Zhao, Phys. Rev. D **71**, 074018 (2005). [arXiv:hep-ph/0501048](#) [hep-ph]
88. S. Jung, H. Murayama, A. Pierce, J.D. Wells, Phys. Rev. D **81**, 015004 (2010). [arXiv:0907.4112](#) [hep-ph]
89. P.H. Frampton, J. Shu, K. Wang, Phys. Lett. B **683**, 294 (2010). [arXiv:0911.2955](#) [hep-ph]
90. J. Shu, T.M.P. Tait, K. Wang, Phys. Rev. D **81**, 034012 (2010)
91. Q.-H. Cao, D. McKeen, J.L. Rosner, G. Shaughnessy, C.E.M. Wagner, Phys. Rev. D **81**, 114004 (2010)
92. I. Dorsner, S. Fajfer, J.F. Kamenik, N. Kosnik, Phys. Rev. D **81**, 055009 (2010). [arXiv:0912.0972](#) [hep-ph]
93. K. Cheung, W.-Y. Keung, T.-C. Yuan, Phys. Lett. B **682**, 287 (2009). [arXiv:0908.2589](#) [hep-ph]
94. A. Djouadi, G. Moreau, F. Richard, R.K. Singh, Phys. Rev. D **82**, 071702 (2010). [arXiv:0906.0604](#) [hep-ph]
95. A. Arhrib, R. Benbrik, C.-H. Chen, Phys. Rev. D **82**, 034034 (2010). [arXiv:0911.4875](#) [hep-ph]
96. Y. Bai, J.L. Hewett, J. Kaplan, T.G. Rizzo, JHEP **1103**, 003 (2011). [arXiv:1101.5203](#) [hep-ph]
97. M.I. Gresham, I.-W. Kim, K.M. Zurek, Phys. Rev. D **83**, 114027 (2011). [arXiv:1103.3501](#) [hep-ph]
98. M.R. Buckley, D. Hooper, J. Kopp, E.T. Neil, Phys. Rev. D **D83**, 115013 (2011)
99. B. Bhattacharjee, S.S. Biswal, D. Ghosh, Phys. Rev. D **83**, 091501 (2011). [arXiv:1102.0545](#) [hep-ph]
100. J. Aguilar-Saavedra, M. Perez-Victoria, JHEP **1105**, 034 (2011). [arXiv:1103.2765](#) [hep-ph]
101. J. Aguilar-Saavedra, M. Perez-Victoria, JHEP **1109**, 097 (2011). [arXiv:1107.0841](#) [hep-ph]
102. R.S. Chivukula, E.H. Simmons, C.-P. Yuan, Phys. Rev. D **82**, 094009 (2010). [arXiv:1007.0260](#) [hep-ph]
103. B. Grinstein, A.L. Kagan, M. Trott, J. Zupan, Phys. Rev. Lett. **107**, 012002 (2011). [arXiv:1102.3374](#) [hep-ph]
104. G. Marques Tavares, M. Schmaltz, Phys. Rev. D **84**, 054008 (2011). [arXiv:1107.0978](#) [hep-ph]
105. S. Jung, A. Pierce, J.D. Wells, Phys. Rev. D **83**, 114039 (2011). [arXiv:1103.4835](#) [hep-ph]
106. Z. Ligeti, G. Marques Tavares, M. Schmaltz, JHEP **1106**, 109 (2011). [arXiv:1103.2757](#) [hep-ph]
107. S.S. Biswal, S. Mitra, R. Santos, P. Sharma, R.K. Singh et al., Phys. Rev. D **86**, 014016 (2012). [arXiv:1201.3668](#) [hep-ph]

108. B.C. Allanach, K. Sridhar, Phys. Rev. D **86**, 075016 (2012)
109. G. Dupuis, J.M. Cline, JHEP **1301**, 058 (2013). [arXiv:1206.1845](#) [hep-ph]
110. J. Aguilar-Saavedra, Phys. Lett. B **736**, 132 (2014). [arXiv:1405.1412](#) [hep-ph]
111. J. Cao, K. Hikasa, L. Wang, L. Wu, J.M. Yang, Phys. Rev. D **D85**, 014025 (2012). [arXiv:1109.6543](#) [hep-ph]
112. S. Fajfer, J.F. Kamenik, B. Melic, JHEP **1208**, 114 (2012). [arXiv:1205.0264](#) [hep-ph]
113. B. Grzadkowski, Z. Hioki, Phys. Lett. B **476**, 87 (2000). [arXiv:hep-ph/9911505](#) [hep-ph]
114. B. Grzadkowski, Z. Hioki, Phys. Lett. B **529**, 82 (2002). [arXiv:hep-ph/0112361](#) [hep-ph]
115. B. Grzadkowski, Z. Hioki, Phys. Lett. B **557**, 55 (2003). [arXiv:hep-ph/0208079](#) [hep-ph]
116. J. Aguilar-Saavedra, R. Herrero-Hahn, Phys. Lett. B **718**, 983 (2013). [arXiv:1208.6006](#) [hep-ph]
117. J. Aguilar-Saavedra, J. Carvalho, N.F. Castro, F. Veloso, A. Onofre, Eur. Phys. J. C **50**, 519 (2007). [arXiv:hep-ph/0605190](#) [hep-ph]
118. E. Boos, L. Dudko, T. Ohl, Eur. Phys. J. C **11**, 473 (1999). [arXiv:hep-ph/9903215](#) [hep-ph]
119. F.d. Águila, J.A. Aguilar-Saavedra, Phys. Rev. D **67**, 014009 (2003)
120. F. Hubaut, E. Monnier, P. Pralavorio, K. Smolek, V. Simak, Eur. Phys. J. C **44S2**, 13 (2005). [arXiv:hep-ex/0508061](#) [hep-ex]
121. M. Mohammadi Najafabadi, J.Phys. G **34**, 39 (2007). [arXiv:hep-ph/0601155](#) [hep-ph]
122. J. Aguilar-Saavedra, Nucl. Phys. B **804**, 160 (2008). [arXiv:0803.3810](#) [hep-ph]
123. M.M. Najafabadi, JHEP **0803**, 024 (2008). [arXiv:0801.1939](#) [hep-ph]
124. J. Aguilar-Saavedra, J. Carvalho, N.F. Castro, A. Onofre, F. Veloso, Eur. Phys. J. C **53**, 689 (2008). [arXiv:0705.3041](#) [hep-ph]
125. J. Aguilar-Saavedra, J. Bernabeu, Nucl. Phys. B **840**, 349 (2010). [arXiv:1005.5382](#) [hep-ph]
126. S.D. Rindani, P. Sharma, Phys. Lett. B **712**, 413 (2012). [arXiv:1108.4165](#) [hep-ph]
127. E. Boos, M. Dubinin, M. Sachwitz, H. Schreiber, Eur. Phys. J. C **16**, 269 (2000). [arXiv:hep-ph/0001048](#) [hep-ph]
128. S. Dutta, A. Goyal, M. Kumar, B. Mellado (2013). [arXiv:1307.1688](#) [hep-ph]
129. Z. Lin, T. Han, T. Huang, J. Wang, X. Zhang, Phys. Rev. D **65**, 014008 (2002). [arXiv:hep-ph/0106344](#) [hep-ph]
130. E. Devetak, A. Nomerotski, M. Peskin, Phys. Rev. D **84**, 034029 (2011). [arXiv:1005.1756](#) [hep-ex]
131. W. Bernreuther, P. Gonzalez, M. Wiebusch, Eur. Phys. J. C **60**, 197 (2009). [arXiv:0812.1643](#) [hep-ph]
132. V.M. Abazov, et al., (D0 Collaboration), Phys. Lett. B **713**, 165 (2012). [arXiv:1204.2332](#) [hep-ex]
133. B. Grzadkowski, M. Misiak, Phys. Rev. D **78**, 077501 (2008). [arXiv:0802.1413](#) [hep-ph]
134. C. Bernardo, N.F. Castro, M.C.N. Fiolhais, H. Gonalves, A.G.C. Guerra et al., Phys. Rev. D **90**(11), 113007 (2014). [arXiv:1408.7063](#) [hep-ph]
135. M. Jezabek, Nucl. Phys. Proc. Suppl. **37B**, 197 (1994). [arXiv:hep-ph/9406411](#) [hep-ph]
136. Prospects for top anti-top resonance searches using early ATLAS data. Tech. Rep. ATL-PHYS-PUB-2010-008, CERN, Geneva (2010)
137. E.L. Berger, Q.-H. Cao, J.-H. Yu, H. Zhang, Phys. Rev. Lett. **109**, 152004 (2012). [arXiv:1207.1101](#) [hep-ph]
138. A. Papaefstathiou, K. Sakurai, JHEP **1206**, 069 (2012). [arXiv:1112.3956](#) [hep-ph]
139. V. Ahrens, A. Ferroglia, M. Neubert, B.D. Pecjak, L.L. Yang, JHEP **1009**, 097 (2010). [arXiv:1003.5827](#) [hep-ph]
140. Q.-H. Cao, B. Yan, J.-H. Yu, C. Zhang (2015). [arXiv:1504.03785](#) [hep-ph]